

DYNAMICS OF SINGULAR COMPLEX ANALYTIC VECTOR FIELDS WITH ESSENTIAL SINGULARITIES II

ALVARO ALVAREZ-PARRILLA*

Grupo Alximia SA de CV
Ensenada, Baja California, CP 22800, México

JESÚS MUCIÑO-RAYMUNDO

Centro de Ciencias Matemáticas
Universidad Nacional Autónoma de México, México

ABSTRACT. Generically, the singular complex analytic vector fields X on the Riemann sphere $\widehat{\mathbb{C}}_z$ belonging to the family

$$\mathcal{E}(r, d) = \left\{ X(z) = \frac{1}{P(z)} e^{E(z)} \frac{\partial}{\partial z} \mid P, E \in \mathbb{C}[z], \deg P = r, \deg E = d \right\},$$

have an essential singularity of finite 1-order at infinity and a finite number of poles on the complex plane. We describe X , particularly the singularity at $\infty \in \widehat{\mathbb{C}}_z$.

In order to do so, we use the natural *correspondence* between $X \in \mathcal{E}(r, d)$, a global singular analytic distinguished parameter $\Psi_X = \int \omega_X$, and the Riemann surface \mathcal{R}_X of the distinguished parameter.

We introduce (r, d) -*configuration trees* Λ_X : combinatorial objects that completely encode the Riemann surfaces \mathcal{R}_X and singular flat metrics associated to $X \in \mathcal{E}(r, d)$. This provides an alternate “dynamical” coordinate system and an analytic classification of $\mathcal{E}(r, d)$. Furthermore, the phase portrait of $\Re(X)$ on \mathbb{C} is decomposed into $\Re(X)$ -invariant regions: half planes and finite height strip flows. The germ of X at $\infty \in \widehat{\mathbb{C}}$ is described as an admissible word (equivalent to certain canonical angular sectors). The structural stability of the phase portrait of $\Re(X)$ is characterized by using Λ_X and the number of topologically equivalent phase portraits of $\Re(X)$ is bounded.

CONTENTS

1. Introduction	2
2. Different facets for singular analytic vector fields $X \in \mathcal{E}(r, d)$	4
3. The geometry of the Riemann surface \mathcal{R}_X	6
4. Combinatorial objects: (r, d) -configuration trees	10
5. Low degree significative examples	11
6. Proof of Main Theorem: description of the family $\mathcal{E}(r, d)$ via combinatorial scheme	18
7. Vieta’s map generalized to transcendental functions	25
8. Decomposition of the phase portraits into invariant components	27
9. On the topology of $\Re(X)$	27
10. Epilogue: the singularity at ∞	29
References	36

1991 *Mathematics Subject Classification.* Primary: 32S65; Secondary: 30F20, 30D30, 32M25.

Key words and phrases. Complex analytic vector fields and Riemann surfaces and Essential singularities.

* Corresponding author.

1. INTRODUCTION

Motivated by the nature of meromorphic and essential singularities of complex analytic vector fields on Riemann surfaces [17], [1], [2], we study the families

$$(1) \quad \mathcal{E}(r, d) = \left\{ X(z) = \frac{1}{P(z)} e^{E(z)} \frac{\partial}{\partial z} \mid P, E \in \mathbb{C}[z], \deg P = r, \deg E = d \right\},$$

of 1-order d vector fields on the Riemann sphere $\widehat{\mathbb{C}}$, generically having an essential singularity at ∞ and r poles on \mathbb{C} .

Each $X \in \mathcal{E}(r, d)$ is provided with a global singular analytic distinguished parameter

$$(2) \quad \Psi_X(z) = \int^z P(\zeta) e^{-E(\zeta)} d\zeta : \widehat{\mathbb{C}}_z \longrightarrow \widehat{\mathbb{C}}_t,$$

which in turn has an associated Riemann surface

$$(3) \quad \mathcal{R}_X = \{(z, \Psi_X(z))\}.$$

Thus there is a correspondence, for $r + d \geq 1$, between

$$(4) \quad X \in \mathcal{E}(r, d) \longleftrightarrow \left\{ \begin{array}{l} \text{branched coverings } \pi_{X,2} : \mathcal{R}_X \longrightarrow (\widehat{\mathbb{C}}_t, \frac{\partial}{\partial t}) \text{ having} \\ d \text{ logarithmic branch points over } \infty, \\ d \text{ logarithmic branch points over } \{a_\sigma\} \subset \mathbb{C}_t, \\ r \text{ ramified branch points over } \{\tilde{p}_\iota\} \subset \mathbb{C}_t \end{array} \right\},$$

where $\pi_{X,2}$ is as in Diagram (8). See also Lemma 3.1, and [1], [2], [3].

The existence of the biholomorphism $(\widehat{\mathbb{C}}_z, X) \cong (\mathcal{R}_X, \pi_{X,2}^*(\frac{\partial}{\partial t}))$ essentially provides a *global flow box* for X , according to Lemma 2.3.

The Riemann surface \mathcal{R}_X associated to Ψ_X can be naturally described by gluing half planes \mathbb{H}^2 and finite height strips $\{0 < \operatorname{Im}(z) < h\}$, and it has its origin on the works of [19], [20], [22], [17], [18], [14], [23].

Three natural cases arise for $X \in \mathcal{E}(r, d)$:

Case $X \in \mathcal{E}(r, 0)$. X has $r \geq 1$ poles (counted with multiplicity) on \mathbb{C}_z and a zero of order $r + 2$ at $\infty \in \widehat{\mathbb{C}}_z$. Ψ_X is a polynomial map. See W. M. Boothby [8], [9] for pioneering work and S. K. Lando et al. [15] chapters 1 and 5 for advances in the combinatorial direction.

Case $X \in \mathcal{E}(0, d)$. X has an isolated essential singularity at $\infty \in \widehat{\mathbb{C}}_z$, no zeros or poles. Ψ_X is an infinitely ramified covering map and $\{\tilde{p}_\iota\} = \emptyset$ in (4). See the seminal works of R. Nevanlinna [19] chapter XI, M. Taniguchi [23]; and [1].

Case $X \in \mathcal{E}(r, d)$. X has $r \geq 1$ poles (counted with multiplicity) on \mathbb{C}_z and an isolated essential singularity at $\infty \in \widehat{\mathbb{C}}_z$. Ψ_X is an infinitely ramified covering map as in (4). This is the *main/generic* case explored in this work.

Obviously, $\mathcal{E}(r, d)$ is an open complex submanifold of \mathbb{C}^{r+d+1} , see (1) and [2]. However for the study of analytical, geometrical and topological aspects of Ψ_X and X , suitable coordinates that shed light on these kind of problems are desirable (recall for instance the role of the critical value $\{c\}$, as useful “coordinates”, in the dynamical study of the quadratic family $\{z \mapsto z^2 + c\}$). In particular, even though the map

$\{\text{coefficients of } P(z), E(z)\} \rightarrow \{\text{critical and asymptotic values } \{\tilde{p}_\iota\} \cup \{a_\sigma\} \text{ of } \Psi_X\}$ is holomorphic, it is insufficient to completely describe the family $\mathcal{E}(r, d)$; see Corollary 1 and example 8.12.3, figures 11 (c), (d) in [1] for an instance in $\mathcal{E}(0, 3)$.

With this in mind, in §4, we introduce (r, d) -configuration trees Λ_X which are combinatorial objects that completely encode the branched Riemann surface \mathcal{R}_X , for $X \in \mathcal{E}(r, d)$. Thus providing explicit “dynamical coordinates” for \mathcal{R}_X , which allows us to obtain a *complete global analytical and geometrical classification* for the family $\mathcal{E}(r, d)$.

The *vertices* of Λ_X are the branch points in \mathcal{R}_X , as in (4), including their ramification index.

The *weighted edges* of Λ_X provide us with two pieces of information:

- 1) each edge specifies which pair of branch points share the same sheet of \mathcal{R}_X ,
- 2) the weight of the edge tells us the relative number of sheets of \mathcal{R}_X , we must go “up or down” on the surface in order to find another sheet containing other branch points.

As a consequence we have:

Main Theorem ((r, d)-configuration trees as parameters for $\mathcal{E}(r, d)$).

There is an isomorphism, as complex manifolds of dimension $r + d + 1$, between $\mathcal{E}(r, d)$ and equivalence classes of (r, d) -configuration trees, i.e.

$$\mathcal{E}(r, d) \cong \{ [\Lambda_X] \mid \Lambda_X \text{ is a } (r, d)\text{-configuration tree} \}.$$

In §5 explicit examples of Λ_X as well as a digression on some of the difficulties encountered in the proof of the Main Theorem, are presented.

The proof is presented in §6, with the description of the equivalence relation and their classes $[\cdot]$ in §6.3.

The Main Theorem provides another characterization of the family $\mathcal{E}(r, d)$ (see [1], [2] and [3]) and enhances the work of A. Speiser [21], R. Nevanlinna [19], [20] p. 291 and G. Elfving [11] on the classification, via line complexes, of (simply connected) Riemann surfaces \mathcal{R}_X related to meromorphic functions Ψ_X .

Provided with the description of \mathcal{R}_X by means of Λ_X , we can now answer the following question:

How can we describe the singularity of X at $\infty \in \widehat{\mathbb{C}}_z$, for $X \in \mathcal{E}(r, d)$?

We ask for a topological/analytical classification of the germs $((\widehat{\mathbb{C}}, \infty), X)$ for $X \in \mathcal{E}(r, d)$. A natural idea is to look at the germ and try to split into a finite union of angular sectors hyperbolic H , elliptic E , parabolic P and entire sectors \mathcal{E} , this last based upon $e^z \frac{\partial}{\partial z}$ at infinity; see Figure 9. Thus obtaining a cyclic word \mathcal{W}_X . Of course this classical idea has its roots in the work of I. Bendixon, A. A. Andronov and F. Dumortier *et al.*; see [4] p. 304, [5] p. 84 and theorem 5.1 in [1].

The following theorem answers the above posed question, as well as the dynamical description of the phase portraits of $\Re(X)$.

Theorem (Dynamical applications). *Let be $X \in \mathcal{E}(r, d)$.*

- 1) *The cyclic word \mathcal{W}_X associated to X at ∞ is recognized as*

$$(5) \quad ((\widehat{\mathbb{C}}_z, \infty), X) \longmapsto \mathcal{W}_X = W_1 W_2 \cdots W_k, \quad W_i \in \{H, E, P, \mathcal{E}\},$$

with exactly $2d$ letters $W_i = \mathcal{E}$.

- 2) *The word \mathcal{W}_X is a complete topological invariant of a germ $((\widehat{\mathbb{C}}, \infty), X)$.*
- 3) *Conversely, a germ of a singular complex analytic vector field $((\mathbb{C}, 0), Y)$ is the restriction of a vector field $X \in \mathcal{E}(r, d)$ at ∞ if and only if*
 - *the point 0 is an isolated essential singularity of Y and*
 - *its admissible word \mathcal{W}_Y satisfies that*
 - i) *the residue of the word $\text{Res}(\mathcal{W}_Y) = 0$,*

- ii) the Poincaré–Hopf index of the word $PH(Y, 0) = 2 + r$,
 - iii) it has exactly $2d$ entire sectors \mathcal{E} .
- 4) The phase portrait of $\Re(X)$ is structurally stable (under perturbations in $\mathcal{E}(r, d)$) if and only if
- X has only simple poles and
 - all edges of Λ_X have weights with a non-zero imaginary component.
- 5) The number of non topologically equivalent phase portraits of $\Re(X)$ is infinite if and only if
- $$(r, d) \in \{(r \geq 2, 1), (r \geq 1, 2), (r \geq 0, d \geq 3)\}.$$

For the accurate assertions and proofs, see Theorem 10.1, Theorem 9.2 and Theorem 9.3 respectively.

A stronger version of the decomposition of the phase portrait into $\Re(X)$ –invariant components, can be found as Theorem 8.1. In particular, for $X \in \mathcal{E}(r, d)$ the Riemann surface \mathcal{R}_X admits an infinite number of half planes \mathbb{H}^2 if and only if $d \geq 1$. However, Example 14 provides a Riemann surface admitting a decomposition in an infinite number of half planes, where the corresponding vector field does not belong to any $\mathcal{E}(r, d)$. Moreover the topological classification of functions Ψ_X is coarser than the classification of phase portraits of vector fields $\Re(X)$, for $\mathcal{E}(r, d)$, see Remark 14.

Diagrammatically, we have

$$X \in \mathcal{E}(r, d) \longleftrightarrow [\Lambda_X] \longrightarrow \underbrace{((\widehat{\mathbb{C}}, \infty), X(z))}_{loc. analytic inv.} \longrightarrow \underbrace{\mathcal{W}_X = W_1 W_2 \cdots W_k}_{loc. topological inv.}.$$

The Main Theorem provides the global, on $\widehat{\mathbb{C}}$, analytic bijection. Moreover, the notion of local invariance makes sense, see §10. For the essential singularity of X at ∞ the analytic/topological nature of the invariant is certainly a novel aspect.

Some of the proofs presented are based upon technical results of [1], however the evidence and examples provided in this work allow for a self contained reading and understanding.

2. DIFFERENT FACETS FOR SINGULAR ANALYTIC VECTOR FIELDS $X \in \mathcal{E}(r, d)$

2.1. Vector fields, differential forms, orientable quadratic differentials, flat metrics, distinguished parameters, Riemann surfaces. We consider the family $\mathcal{E}(r, d)$ as in (1).

Let $X \in \mathcal{E}(r, d)$ be a vector field, we denote by $\mathcal{P} = \{p_\ell\}$ the set of poles of X . The associated singular analytic differential form

$$(6) \quad \omega_X = P(z) e^{-E(z)} dz,$$

is such that $\omega_X(X) \equiv 1$.

A singular analytic quadratic differential \mathcal{Q} on $\widehat{\mathbb{C}}_z$ is *orientable* if it is globally given as $\mathcal{Q} = \omega \otimes \omega$, for some singular analytic differential form ω on $\widehat{\mathbb{C}}_z$. In particular,

$$(7) \quad \mathcal{Q}_X = \omega_X \otimes \omega_X = P^2(z) e^{-2E(z)} dz^2.$$

The singular horizontal foliation of \mathcal{Q}_X on $\mathbb{C}_z \setminus \mathcal{P}$ corresponds to the trajectories of the real vector field $\Re(X)$, see for instance (2.2) of [1].

Since ω_X is holomorphic on \mathbb{C}_z , the local notion of *distinguished parameter*, see [22] p. 20, can be extended as follows.

Definition 2.1. The map

$$\Psi_X(z) = \int_{z_0}^z P(\zeta) e^{-E(\zeta)} d\zeta : \mathbb{C}_z \longrightarrow \widehat{\mathbb{C}}_t$$

is a *global distinguished parameter* for X (note the dependence on $z_0 \in \mathbb{C}_z$).

A *singular flat metric* g_X with singular set $\mathcal{P} \subset \mathbb{C}_z$ is the flat Riemannian metric on $\mathbb{C}_z \setminus \mathcal{P}$ defined as the pullback under $\Psi_X : (\mathbb{C}_z, g_X) \rightarrow (\mathbb{C}_t, \delta)$, where δ is the usual flat metric on \mathbb{C}_t . The singularities of g_X at $p_\ell \in \mathcal{P}$ are cone points with angle $(2\mu_\ell + 2)\pi$, where $-\mu_\ell \leq -1$ is the order of the pole p_ℓ of X . Then the trajectories of $\Re(X)$ and $\Im(X)$ are unitary geodesics in $(\mathbb{C}_z \setminus \mathcal{P}, g_X)$.

The graph of Ψ_X

$$\mathcal{R}_X = \{(z, t) \mid t = \Psi_X(z)\} \subset \mathbb{C}_z \times \widehat{\mathbb{C}}_t$$

is a Riemann surface. The flat metric¹ on $(\mathcal{R}_X, \pi_{X,2}^*(\frac{\partial}{\partial t}))$ is induced by the usual metric on $(\widehat{\mathbb{C}}_t, \delta)$, equivalently $(\widehat{\mathbb{C}}_t, \frac{\partial}{\partial t})$, via the projection of $\pi_{X,2}$, and coincides with $g_X = \Psi_X^*(\delta)$ since $\pi_{X,1}$ is an isometry.

Lemma 2.2. *The following diagram commutes*

$$(8) \quad \begin{array}{ccc} (\widehat{\mathbb{C}}_z, X) & \xleftarrow{\pi_{X,1}} & (\mathcal{R}_X, \pi_{X,2}^*(\frac{\partial}{\partial t})) \\ \searrow \Psi_X & & \downarrow \pi_{X,2} \\ & & (\widehat{\mathbb{C}}_t, \frac{\partial}{\partial t}) \end{array}$$

Moreover, $\pi_{X,1}$ is a biholomorphism between $(\mathcal{R}_X, \pi_{X,2}^*(\frac{\partial}{\partial t}))$ and (\mathbb{C}_z, X) . \square

In contrast, for a rational vector field with simple zeros, the associated $\pi_{X,1}$ is not a biholomorphism between $(\mathcal{R}_X, \pi_{X,2}^*(\frac{\partial}{\partial t}))$ and (\mathbb{C}_z, X) , since Ψ_X is multivalued. In what follows, unless explicitly stated, we shall use the abbreviated form \mathcal{R}_X instead of the more cumbersome $(\mathcal{R}_X, \pi_{X,2}^*(\frac{\partial}{\partial t}))$, see Figures 1 and 2.

In Diagram (8) we abuse notation slightly by saying that the domain of Ψ_X is $\widehat{\mathbb{C}}_z$. This is a delicate issue, see Remark 1.1 following Proposition 1.

Lemma 2.3. 1. The map Ψ_X is a global flow box of X , i.e.

$$(\Psi_X)_* X = \frac{\partial}{\partial t} \quad \text{on the whole } \mathbb{C}_z.$$

2. For fixed $z_0 \in \mathbb{C}_z \setminus \mathcal{P}$, the maximal (under analytic continuation) time domain of the local flow of X is

$$\pi_{X,1}(\cdot) = \varphi(z_0, \cdot) : \Omega_X = \mathcal{R}_X \setminus \cup_{p_\ell \in \mathcal{P}} \{(p_\ell, \tilde{p}_\ell)\} \longrightarrow \mathbb{C}_z \setminus \mathcal{P}.$$

\square

2.2. The singular complex analytic dictionary.

Proposition 1 (Dictionary between the singular analytic objects originating from $X \in \mathcal{E}(r, d)$, [1]). *The following diagram describes a canonical one-to-one correspondence between its objects*

¹ $(\widehat{\mathbb{C}}_z, X)$ denotes a pair, Riemann sphere and a singular complex analytic vector field.
 $((\mathbb{C}_z, z_0), X)$ denotes a germ of singular

$$\begin{array}{ccc}
& X(z) = \frac{1}{P(z)} e^{E(z)} \frac{\partial}{\partial z} & \\
\swarrow & & \searrow \\
\omega_X(z) = P(z) e^{-E(z)} dz & & \Psi_X(z) = \int^z P(\zeta) e^{-E(\zeta)} d\zeta_X \\
\downarrow & & \downarrow \\
\omega_X \otimes \omega_X(z) & & (\mathcal{R}_X, \pi_{X,2}^*(\frac{\partial}{\partial t})) \\
\swarrow & & \searrow \\
((\mathbb{C}, g_X), \mathfrak{Re}(X)) & &
\end{array}
\tag{9}$$

Remark 1. 1. The choice of initial and end points z_0, z for the integral defining Ψ_X can be relaxed to include $\infty \in \widehat{\mathbb{C}}_z$ by integrating along asymptotic paths associated to asymptotic values of Ψ_X at the essential singularity $\infty \in \widehat{\mathbb{C}}_z$, see §5.
2. \mathcal{R}_X are non compact translation surfaces, following [25] §3.3 and [16].

3. THE GEOMETRY OF THE RIEMANN SURFACE \mathcal{R}_X

3.1. Branch points of \mathcal{R}_X : local ramification data. For $X \in \mathcal{E}(r, d)$, the distinguished parameter Ψ_X belongs to the family

$$(10) \quad SF_{r,d} = \left\{ \int_0^z P(\zeta) e^{-E(\zeta)} d\zeta + b \mid P, E \in \mathbb{C}[z], \deg P = r, \deg E = d \right\},$$

of structurally finite entire functions of type (r, d) . In order to determine the Riemann surface \mathcal{R}_X precisely, one needs the knowledge of the branch points $\{(z_a, t_a)\} \subset \mathcal{R}_X$ under $\pi_{X,2}$, see [19] chap XI, [23], [24] and [1].

Lemma 3.1 (The existence of logarithmic and finitely ramified branch points). *Let $\Psi_X : \mathbb{C}_z \rightarrow \widehat{\mathbb{C}}_t$ be a structurally finite entire function of type (r, d) , with $d \geq 1$. Then*

- 1) Ψ_X has r critical values $\{\tilde{p}_i\} \subset \mathbb{C}_t$ (counted with multiplicity),
 - 2) Ψ_X^{-1} has d direct singularities corresponding to d logarithmic branch points over d finite asymptotic values $\{a_\sigma\} \subset \widehat{\mathbb{C}}_t$, and
 - 3) Ψ_X^{-1} has d direct singularities corresponding to d logarithmic branch points over $\infty \in \widehat{\mathbb{C}}_t$,
- Furthermore, Ψ_X^{-1} has no indirect singularities.

Proof. Case $(r, 0)$ is elementary. Case (r, d) with $d \geq 1$ can be found as lemma 8.4 in [1] with a proof that relies heavily on the work of M. Taniguchi [23], [24]. \square

Remark 2. To be precise, the logarithmic branch points associated to the isolated singularity at $\infty \in \widehat{\mathbb{C}}_z$, are not in fact in $\mathcal{R}_X \subset \widehat{\mathbb{C}}_z \times \widehat{\mathbb{C}}_t$. Instead, see for instance [7], they lie on the non-Hausdorff closure $\overline{\mathbb{C}}_z \times \widehat{\mathbb{C}}_t$ of $\mathbb{C}_z \times \widehat{\mathbb{C}}_t$. Here

$$(11) \quad \overline{\mathbb{C}}_z := \left((\widehat{\mathbb{C}} \times \{1\}) \sqcup (\widehat{\mathbb{C}} \times \{2\}) \sqcup \cdots \sqcup (\widehat{\mathbb{C}} \times \{2d\}) \right) / \sim$$

is the *sphere with $2d$ infinities*, that is the disjoint union of $2d$ copies of the Riemann sphere $\widehat{\mathbb{C}}$ with the equivalence relation \sim , given by $(z, \sigma) \sim (z, \rho)$ for all $\sigma, \rho \in \{1, \dots, 2d\}$ if $z \neq \infty$.

We will denote the $2d$ distinct infinities, referred to in Lemma 3.1, by $\{\infty_\sigma\}_{\sigma=1}^{2d} \subset \overline{\mathbb{C}}_z$.

Suitable coordinate pairs

$$(z_\vartheta, t_\vartheta) \in \mathcal{R}_X \subset \overline{\mathbb{C}}_z \times \widehat{\mathbb{C}}_t$$

will be identified with the branch points of \mathcal{R}_X . In what follows, the reader might find it helpful to follow along with Figures 1–6 in §5.1.

1) For $r \geq 1$, $p_\iota \in \mathbb{C}_z$ is a **pole** of X (zero of ω_X) if and only if its image $\tilde{p}_\iota = \Psi_X(p_\iota) \in \mathbb{C}_t$ is a critical value of Ψ_X . Moreover $(p_\iota, \tilde{p}_\iota) \in \mathcal{R}_X$ is a finitely ramified branch point (under $\pi_{X,2}$) with ramification index $\mu_\iota + 1 \geq 2$, where $-\mu_\iota \leq -1$ is the order of the pole p_ι .

We enumerate the corresponding finitely ramified branch points in \mathcal{R}_X as

$$(12) \quad \{(p_\iota, \tilde{p}_\iota)\}_{\iota=1}^n \subset \mathcal{R}_X, \text{ with order } -\mu_\iota \leq -1 \text{ and } \sum_{\iota=1}^n \mu_\iota = r.$$

For $d \geq 1$, $\infty \in \widehat{\mathbb{C}}_z$ is an **isolated essential singularity of X** . Lemma 3.1 allows us to denote the distinct finite asymptotic values by

$$(13) \quad \{a_j\}_{j=1}^m \subset \mathbb{C}_t, \text{ with multiplicities } \{\nu_j\}_{j=1}^m \text{ and } \sum_{j=1}^m \nu_j = d.$$

Thus, $\pi_{X,2}^{-1}(a_j)$ should contain at least one logarithmic branch point of \mathcal{R}_X for each exponential tract associated to the finite asymptotic value a_j ; see [7] p. 356 where exponential tracts are denoted $U(r)$ and [10] p. 212. In other words, if $\alpha(\tau)$ is an asymptotic path approaching $\infty_\sigma \in \overline{\mathbb{C}}_z$ associated to the finite asymptotic value a_j then we may assume that $\alpha(\tau)$ is restricted to one exponential tract (the one containing $\infty_\sigma \in \overline{\mathbb{C}}_z$) and

$$\lim_{\tau \rightarrow \infty} \Psi_X(\alpha(\tau)) = a_j.$$

Hence, the exponential tracts $\{\alpha\}$ serve as indices for the accurate description of the $2d$ logarithmic branch points in \mathcal{R}_X .

2) We will denote the corresponding logarithmic branch points over the finite asymptotic values $a_{j(\sigma)} \in \mathbb{C}_t$, by

$$(14) \quad (\infty_\sigma, a_{j(\sigma)}) \in \mathcal{R}_X, \text{ for } \sigma \in \{1, \dots, d\}.$$

3) To be precise, the d logarithmic branch points over $\infty \in \widehat{\mathbb{C}}_t$ will be denoted by

$$(15) \quad (\infty_\sigma, \infty) \in \mathcal{R}_X, \text{ for } \sigma \in \{d+1, \dots, 2d\}.$$

Recalling that the finite asymptotic value a_j has multiplicity ν_j , the correspondence between indices is given by

$$(16) \quad j = j(\sigma) \in \underbrace{1, \dots, \nu_1}_1, \underbrace{\nu_1 + 1, \dots, \nu_1 + \nu_2}_2, \dots, \underbrace{d - \nu_m + 1, \dots, d}_m,$$

where σ enumerates the logarithmic branch points $b_\sigma \in \mathcal{R}_X$ and the exponential tracts $\alpha = \alpha(\sigma) := \sigma$, while $j = j(\sigma)$ enumerates the distinct finite asymptotic values $a_j \in \mathbb{C}_t$.

Remark 3. We can assign a unique $\mu_\vartheta \in \mathbb{N} \cup \{0, \infty\}$ which denotes the ramification index minus one of $b_\vartheta = (z_\vartheta, t_\vartheta) \in \mathcal{R}_X$. Therefore, the assignment

$$(17) \quad X \longmapsto \sum_{\iota=1}^n (p_\iota, \tilde{p}_\iota, -\mu_\iota) + \sum_{\sigma=1}^d (\infty_\sigma, a_\sigma, \infty) \doteq \sum_{t \in \widehat{\mathbb{C}}_t} \sum_{\vartheta} (z_\vartheta, t_\vartheta, \mu_\vartheta),$$

can be thought as an *ad hoc notion of divisor* of $\pi_{X,2}$. The above discussion can be summarized in Table 1.

TABLE 1. Branch points of \mathcal{R}_X .

Point in \mathcal{R}_X $b_\theta = (z_\theta, t_\theta)$	Triad $(z_\theta, t_\theta, \mu_\theta)$	Notation & meaning
$(p_\iota, \tilde{p}_\iota)$ (12)	$\textcircled{\iota} = (p_\iota, \tilde{p}_\iota, -\mu_\iota)$	Pole vertices; $\tilde{p}_\iota = \Psi_X(p_\iota)$ is a critical value of Ψ_X , p_ι is a pole of X having order $-\mu_\iota \leq -1$, hence $(p_\iota, \tilde{p}_\iota)$ is a branch point with ramification index $\mu_\iota + 1 \geq 2$.
$(\infty_\sigma, a_\sigma)$ (14)	$\textcircled{\sigma} = (\infty_\sigma, a_\sigma, \infty)$	Essential vertices; $\infty \in \widehat{\mathbb{C}}_z$ is an essential singularity of X , $a_\sigma \in \mathbb{C}_t$ being a finite asymptotic value of Ψ_X , with exponential tract α_σ , so $(\infty_\sigma, a_\sigma)$ is a logarithmic branch point in the closure of $\mathcal{R}_X \subset \overline{\mathbb{C}}_z \times \widehat{\mathbb{C}}_t$.

Note that (15) does not appear in (17) or Table 1 since it will not be needed.

Lemma 3.2. *Let $X \in \mathcal{E}(r, d)$. The associated Ψ_X has exactly one finite asymptotic or finite critical value $t_1 \in \mathbb{C}_t$ if and only if*

$$(r, d) = \begin{cases} (r \geq 1, 0) & \text{and } X \text{ has a unique pole of order } -r, \\ & \text{in which case } t_1 \text{ is the critical value,} \\ (0, 1) & \text{and } X \text{ has an isolated essential singularity at } \infty \in \widehat{\mathbb{C}}_z, \\ & \text{in which case } t_1 \text{ is the finite asymptotic value.} \end{cases}$$

Proof. (\Leftarrow) When $(r, d) = (0, 1)$, $\Psi_X(z) = \int^z e^{a\zeta+b} d\zeta$, $t_1 = a_1$, see example 4.16 or equation (8.19) in [1]. In the case $(r, d) = (r \geq 1, 0)$, the required distinguished parameter is $\Psi_X(z) = \int^z (\zeta - p)^r d\zeta$.

(\Rightarrow) By Lemma 3.1, Ψ_X^{-1} has d logarithmic branch points over d finite asymptotic values, d logarithmic branch points over $\infty \in \widehat{\mathbb{C}}_t$ and r critical values (with multiplicity). Let $\{(z_a, t_a)\} \subset \pi_{X,2}^{-1}(t_0) \subset \mathcal{R}_X$ be all the branch points over t_0 . The set $\{(z_a, t_a)\}$ consists of exactly d logarithmic branch points over t_0 and $n \leq r$ finitely ramified branch points (p_ι, t_ι) of ramification indices $\mu_\iota + 1$ with $r = \sum_{\iota=1}^{n \leq r} \mu_\iota$. We proceed by contradiction: suppose that $d + n \geq 2$. Then \mathcal{R}_X has $d + n$ connected components: d arising from the logarithmic branch points and n arising from the finitely ramified branch points. However, \mathcal{R}_X is biholomorphic to $\widehat{\mathbb{C}}$, which of course consists of only one connected component. Thus $d + n = 1$ which immediately implies both cases. \square

3.2. The Riemann surface \mathcal{R}_X described by glueing sheets.

Definition 3.3. Let $\{t_k\}_{k=1}^r \subset \mathbb{C}_t$ be a finite set of different points. A *sheet* is a copy of \mathbb{C}_t with $r \geq 1$ branch cuts L_k ; i.e. \mathbb{C}_t is cut along horizontal right segments

$L_k = [t_k, \infty)$, remaining connected, but with $2r$ horizontal boundaries (left there for further isometric glueing²)

$$(18) \quad \mathbb{C}_t \setminus \{L_k\}_{k=1}^r \cong [\mathbb{C}_t \setminus (\cup_{k=1}^r [t_k, \infty))] \cup_{k=1}^r \{[t_k, \infty)_+, [t_k, \infty)_-\},$$

where the subindices \pm refer to the obvious upper or lower boundary using $\text{Im}(t)$. We say that the *height of the cut* L_k is $\text{Im}(t_k)$. Note that cuts (and the corresponding boundaries) need not be to the right, they could be more general simple curves, however for notational simplicity, (18) is written using right cuts $[t_k, \infty)_\pm$ only.

A *diagonal of the sheet* $\mathbb{C}_t \setminus \{L_k\}_{k=1}^r$ is an oriented straight line segment

$$(19) \quad \Delta_{\sigma\rho} = \overline{t_\sigma t_\rho} \subset \mathbb{C}_t \setminus \{L_k\}_{k=1}^r,$$

starting at t_σ and ending at t_ρ , here $\sigma, \rho \in \{1, \dots, r\}$.

See Figures 1, 2 and 3 for examples of Riemann surfaces constructed as in Definition 3.3 and Figures 1 and 3 for examples of diagonals.

Noticing that sheets in turn can be decomposed further into *elementary building blocks*, we make the following.

Definition 3.4. A *(closed) half plane* is the pair $(\bar{\mathbb{H}}_\pm^2, \frac{\partial}{\partial t})$.

A *(closed) finite height horizontal strip*, is $(\{0 \leq \text{Im}(t) \leq h\}, \frac{\partial}{\partial t})$. Note that diagonals are directly related to finite height horizontal strips.

Similarly logarithmic and finitely ramified branch points in \mathcal{R}_X give rise to the following non elementary building blocks.

A *semi-infinite helicoid* is

$$\left((\bar{\mathbb{H}}_\pm^2 \cup \bar{\mathbb{H}}_\mp^2 \cup \dots), \frac{\partial}{\partial t} \right)$$

glued together along their boundaries as in the graph of $\Psi_X(z) = \exp(-z)$, see Diagram (8).

A *finite helicoid* is an even finite succession of half-planes

$$\left((\bar{\mathbb{H}}_\pm^2 \cup \bar{\mathbb{H}}_\mp^2 \cup \dots \cup \bar{\mathbb{H}}_\mp^2), \frac{\partial}{\partial t} \right).$$

3.3. Relative position of the branch points on \mathcal{R}_X . In order to completely describe \mathcal{R}_X we also require information of the relative position of the branch points $\{(z_a, t_a)\}$ on the surface.

Definition 3.5. Let $t_a, t_r \in \{a_1, \dots, a_m, \tilde{p}_1, \dots, \tilde{p}_n\} \subset \mathbb{C}_t$ be two distinct (finite) asymptotic or critical values of Ψ_X and consider the oriented straight line segment $\overline{t_a t_r} \subset \mathbb{C}_t$. The inverse image $\pi_{X,2}^{-1}(\overline{t_a t_r}) = \{\Delta_{\vartheta ar}\} \subset \mathcal{R}_X$ is a set consisting of a finite (when $m = 0$, equivalently $d = 0$) or an infinite (when $m \geq 1$) number of copies of $\overline{t_a t_r}$. For each segment $\Delta_{\vartheta ar}$, let $\delta_{\vartheta ar} = \pi_{X,1}(\Delta_{\vartheta ar}) \subset \overline{\mathbb{C}_z}$.

1) A segment $\Delta_{\vartheta ar} \subset \mathcal{R}_X$ is a *diagonal* of \mathcal{R}_X , when the interior³ of $\delta_{\vartheta ar}$ is in \mathbb{C}_z and $\delta_{\vartheta ar}$ has its endpoints $z_a, z_r \in \mathcal{P} \cup \{\infty_1, \dots, \infty_d\} \subset \overline{\mathbb{C}_z}$.

2) Moreover, for a given diagonal $\Delta_{\vartheta ar}$, the two endpoints b_a, b_r of $\Delta_{\vartheta ar}$ share the same sheet $\mathbb{C}_{\Delta_{\vartheta ar}} \setminus \{\text{suitable branch cuts}\}$ in \mathcal{R}_X .

Remark 4. By notation if we drop the index ϑ from $\Delta_{\vartheta ar}$ we are specifying a particular diagonal Δ_{ar} .

The diagonals Δ_{ar} have endpoints as follows:

² As is usual in the isometric framework, for details see corollary 5.11 of [1].

³Since $\delta_{\vartheta ar}$ is a path homeomorphic to $[a, b] \subset \mathbb{R}$, by the *interior* of $\delta_{\vartheta ar}$ we mean the preimage, under the homeomorphism, of (a, b) .

- 1) $\Delta_{\iota\kappa}$ has as endpoints two pole vertices $(p_\iota, \tilde{p}_\iota)$ and $(p_\kappa, \tilde{p}_\kappa)$, $\iota \neq \kappa$. For an example see middle column of Figure 1 in §5.1.
- 2) $\Delta_{\iota\sigma}$ has as endpoints a pole vertex and an essential vertex $(p_\iota, \tilde{p}_\iota)$ and $(\infty_\sigma, a_\sigma)$, see equation (16) for the subindices. For an example see middle column of Figure 3 in §5.1.
- 3) $\Delta_{\sigma\rho}$ has as endpoints two essential vertices with finite asymptotic values a_σ and a_ρ with exponential tracts α_σ and α_ρ : $(\infty_\sigma, a_\sigma)$ to (∞_ρ, a_ρ) , $\sigma \neq \rho$, where the subindices are as in (16). For an example see right hand side of Figure 5 in §5.1.

For $\Delta_{\alpha\tau}$ a diagonal associated to the finite asymptotic or critical values t_α and t_τ , note that $\pi_{X,1}(\Delta_{\alpha\tau})$ has its endpoints $z_\alpha, z_\tau \in \mathcal{P} \cup \{\infty_1, \dots, \infty_d\} \subset \overline{\mathbb{C}}_z$ and since $(z_\tau, t_\tau), (z_\alpha, t_\alpha) \in \mathcal{R}_X$, the associated semi-residue is

$$(20) \quad S(\omega_X, z_\alpha, z_\tau, \delta_{\alpha\tau}) = \int_{\pi_{X,1}(\Delta_{\alpha\tau})} \omega_X = t_\tau - t_\alpha.$$

In other words, an oriented straight line segment $\Delta_{\alpha\tau}$ in \mathcal{R}_X is equivalent to the number $t_\tau - t_\alpha$ in \mathbb{C}^* .

Lemma 3.6 (Existence of diagonals in \mathcal{R}_X). *Suppose that there are at least two branch points $\{(z_\alpha, t_\alpha)\} \subset \mathcal{R}_X$, with $t_\alpha \in \mathbb{C}$.*

Then every branch point (z_α, t_α) is an endpoint for at least one diagonal.

Proof. Consider any branch point $(z_\alpha, t_\alpha) \in \pi_{X,2}^{-1}(t_\alpha)$, with $t_\alpha \in \{a_1, \dots, a_m, \tilde{p}_1, \dots, \tilde{p}_n\} \subset \mathbb{C}_t$. Suppose that there is no diagonal $\Delta_{\alpha\tau}$ with endpoint (z_α, t_α) . This implies that (z_α, t_α) does not share a sheet, $\mathbb{C}_t \setminus \{\text{suitable branch cuts}\}$, with any other branch point $(z_\tau, t_\tau) \in \pi_{X,2}^{-1}(t_\tau)$, for some finite asymptotic or critical value $t_\tau \neq t_\alpha$ (note that the existence of t_τ is guaranteed by Lemma 3.2). In other words the only sheets, $\mathbb{C}_t \setminus \{\text{suitable branch cuts}\}$, of \mathcal{R}_X containing the branch point (z_α, t_α) are of the form $\mathbb{C}_t \setminus \{L_\alpha\}$, for $L_\alpha = [t_\alpha, \infty)$, hence by the same arguments as in Lemma 3.2, \mathcal{R}_X will have at least 2 connected components (one containing (z_α, t_α) and the other containing (z_τ, t_τ)), leading to a contradiction. \square

4. COMBINATORIAL OBJECTS: (r, d) -CONFIGURATION TREES

Denote the universal cover of \mathbb{C}^* by $\widetilde{\mathbb{C}}^* = \{|z|e^{i\arg(z)}\}$, where $\arg(z)$ is the multivalued argument. For $r + d \geq 1$ we have the following.

Definition 4.1. A (r, d) -configuration tree is a graph tree $\Lambda = \{V; E\}$ with:

- $d + n$ vertices

$$V = \left\{ \textcircled{1} = \underbrace{(p_\iota, \tilde{p}_\iota, -\mu_\iota)}_{\text{pole vertex}} \right\}_{\iota=1}^n \bigcup \left\{ \textcircled{2} = \underbrace{(\infty_\sigma, a_\sigma, \infty)}_{\text{essential vertex}} \right\}_{\sigma=1}^d = \left\{ \textcircled{a} = (z_\alpha, t_\alpha, \mu_\alpha) \right\}_{\alpha=1}^{d+n}$$

where $z_\alpha \in \overline{\mathbb{C}}_z$, $t_\alpha \in \widehat{\mathbb{C}}_t$, $\mu_\alpha \in \mathbb{N} \cup \{\infty\}$, $\sum_{\iota=1}^n \mu_\iota = r$; and

- $d + n - 1$ weighted edges

$$E = \{(\Delta_{\alpha\tau}, \tilde{\lambda}_{\alpha\tau}) \mid \Delta_{\alpha\tau} \text{ starts at } \textcircled{a} \text{ and ends at } \textcircled{2}, \tilde{\lambda}_{\alpha\tau} \in \widetilde{\mathbb{C}}^*\}.$$

In addition, the following conditions on the number $d + n$ of vertices must be satisfied:

If Λ consists of only one vertex, then

$$\text{the } (r, 0)\text{-configuration trees are } \left\{ \textcircled{1} = (p_1, \tilde{p}_1, -r); \emptyset \right\},$$

the $(0, 1)$ -configuration trees are $\{\textcircled{1} = (\infty_1, a_1, \infty); \emptyset\}$.

If Λ has at least two vertices, then:

- 1) *Existence of edges.* There are no edges between vertices $\textcircled{a} = (z_a, t_a, \mu_a)$ and $\textcircled{r} = (z_r, t_r, \mu_r)$ for $t_a = t_r$.
- 2) *Weight of an edge.* When an edge Δ_{ar} exists its associated weight is

$$(21) \quad \tilde{\lambda}_{ar} = (t_r - t_a) e^{i2\pi K(a,r)} = |t_r - t_a| e^{i\arg_0(t_r - t_a) + i2\pi K(a,r)} \in \widetilde{\mathbb{C}}^*,$$

where $K(a, r) \in \mathbb{Z}$.

- 3) *Minimality condition.* There are at least two vertices, say $\textcircled{1} = (z_1, t_1, \mu_1)$ and $\textcircled{3} = (z_3, t_3, \mu_3)$ with $t_1 \neq t_3$, such that there is an edge Δ_{13} connecting them. The respective weight⁴ satisfies

$$\lambda_{13} = t_3 - t_1 \in \mathbb{C}^*, \text{ i.e. } K(1, 3) = 0.$$

- 4) *Preferred horizontal subtree.* The edges $\{(\Delta_{ar}, \tilde{\lambda}_{ar})\}$ with $\tilde{\lambda}_{ar} \in \mathbb{C}^*$ form a finite set of connected *horizontal* subtrees $\{\Lambda_H\}$. On each horizontal subtree $\Lambda_H = \{\{\textcircled{a}\}; \{(\Delta_{ar}, \tilde{\lambda}_{ar})\}\}$ we require that $t_3 \notin \{t \in \mathbb{C} \mid \operatorname{Im}(t_a) < \operatorname{Im}(t) < \operatorname{Im}(t_r)\}$ for each vertex $\textcircled{3} \in \Lambda_H$ not an endpoint of an edge $\Delta_{ar} \in \Lambda_H$ not having as endpoints $\textcircled{3}$ (i.e. $\textcircled{3} \neq \textcircled{a}, \textcircled{r}$).

Remark 5. When $r = 0$, this definition reduces to the definition of a d -configuration tree presented in §8.3 of [1]. The equivalence becomes explicit by observing that the essential vertices $(\infty_\sigma, a_\sigma, \infty)$ of $(0, d)$ -configuration trees correspond to the vertices $(\infty_\sigma, a_\sigma)$ of d -configuration trees.

Remark 6. Note that (r, d) -configuration trees are *oriented, traversable* trees.

1. The orientation of the edge Δ_{ar} coincides with the orientation of the line segment $\overline{t_a t_r}$.
2. The vertex $\textcircled{1}$ will be called the starting vertex for the traversal of the (r, d) -configuration tree.

5. LOW DEGREE SIGNIFICATIVE EXAMPLES

Example 1. Consider the vector field

$$X(z) = \frac{1}{(z-p_1)^{\mu_1}(z-p_2)^{\mu_2}} \frac{\partial}{\partial z}, \quad p_1, p_2 \in \mathbb{C}_z, \quad p_1 \neq p_2, \quad \mu_1 + \mu_2 = r, \quad \mu_1, \mu_2 \geq 1,$$

and its distinguished parameter

$$\Psi_X(z) = \int_{z_0}^z (\zeta - p_1)^{\mu_1} (\zeta - p_2)^{\mu_2} d\zeta.$$

In this case the $(r, 0)$ -configuration tree has two pole vertices and one edge

$$\Lambda_X = \{\textcircled{1} = (p_1, \tilde{p}_1, -\mu_1), \textcircled{2} = (p_2, \tilde{p}_2, -\mu_2); (\Delta_{12}, \lambda_{12})\},$$

where $\tilde{p}_j = \Psi_X(p_j)$, for $j = 1, 2$, are the critical values and the weight λ_{12} is the semi-residue $S(\omega_X, p_1, p_2, \gamma) = \tilde{p}_2 - \tilde{p}_1$, according to (20). See Figure 1.

Example 2. Consider the vector field

$$X(z) = \lambda^{-1} e^z \frac{\partial}{\partial z}, \quad \text{with } \lambda \in \mathbb{C}^*,$$

and its distinguished parameter

$$\Psi_X(z) = \int_{z_0}^z \omega_X = \lambda(e^{-z_0} - e^{-z}).$$

We then have an isolated essential singularity at $\infty \in \widehat{\mathbb{C}}_z$ with finite asymptotic value

⁴ In order to make it easier to describe the geometry of the Riemann surfaces \mathcal{R}_X , it will be convenient to sometimes use λ_{ar} instead of $\tilde{\lambda}_{ar}$ to emphasize that the argument lies in $[0, 2\pi)$.

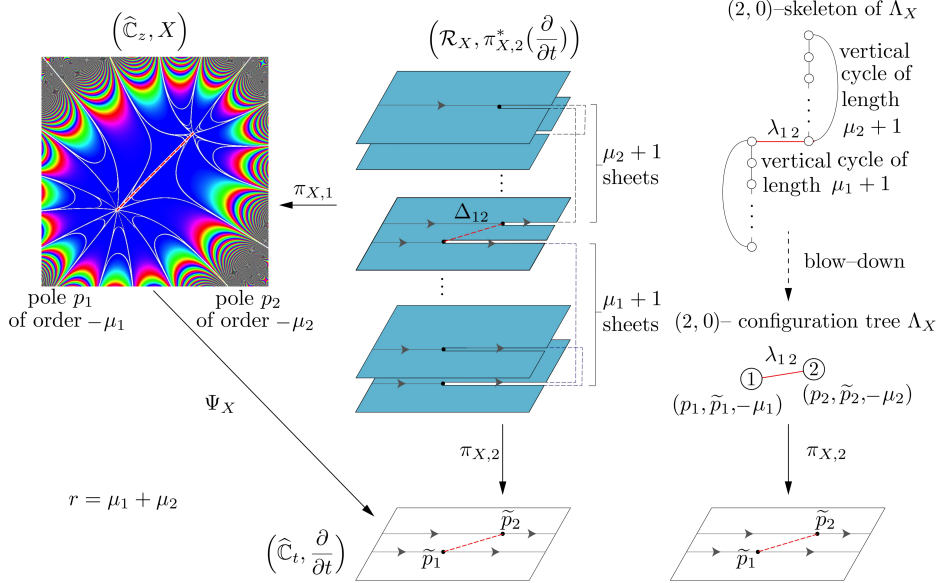


FIGURE 1. Vector field $\frac{1}{(z-p_1)^{\mu_1}(z-p_2)^{\mu_2}} \frac{\partial}{\partial z}$ with two poles p_ℓ of order $-\mu_\ell$. The diagonal $\Delta_{12} \subset \mathcal{R}_X$ associated to the finitely ramified branch points and its projections via $\pi_{X,1}$ and $\pi_{X,2}$ are coloured red. The phase portrait (left drawing) is the case with poles of orders $-\mu_1 = 5$ and $-\mu_2 = 3$. See Example 1, and §6.2 for the drawing on the right.

$$a_1 = \Psi_X(\infty) = \lambda e^{-z_0}.$$

The $(0,1)$ -configuration tree consists of one essential vertex and no edges

$$\Lambda_X = \{(1) = (\infty_1, a_1, \infty); \emptyset\}.$$

See Figure 2.

Example 3. Consider the vector field

$$X(z) = \frac{e^z}{\lambda(z-p_1)} \frac{\partial}{\partial z}, \text{ with } \lambda \in \mathbb{C}^* \text{ and } p_1 \in \mathbb{C}_z,$$

and its distinguished parameter

$$\Psi_X(z) = \int_{z_0}^z \omega_X = \lambda(e^{-z_0}(z_0 - p_1 + 1) - e^{-z}(z - p_1 + 1)).$$

Once again we have an isolated essential singularity at $\infty \in \widehat{\mathbb{C}}_z$ with finite asymptotic value

$$a_1 = \Psi_X(\infty) = \lambda e^{-z_0}(z_0 - p_1 + 1)$$

corresponding to the exponential tract $\{z \in \mathbb{C}_z \mid \Re(z) > 0\}$, and the pole p_1 has an associated critical value

$$\tilde{p}_1 = \Psi_X(p_1) = \lambda(e^{-z_0}(z_0 - p_1 + 1) - e^{-p_1}).$$

The $(1,1)$ -configuration tree has an essential vertex, a pole vertex and one edge

$$\Lambda_X = \{(1) = (\infty_1, a_1, \infty), (2) = (p_1, \tilde{p}_1, -1); (\Delta_{12}, \lambda_{12})\},$$

with weight $\lambda_{12} = \tilde{p}_1 - a_1 = -\lambda e^{-p_1}$. See Figure 3.

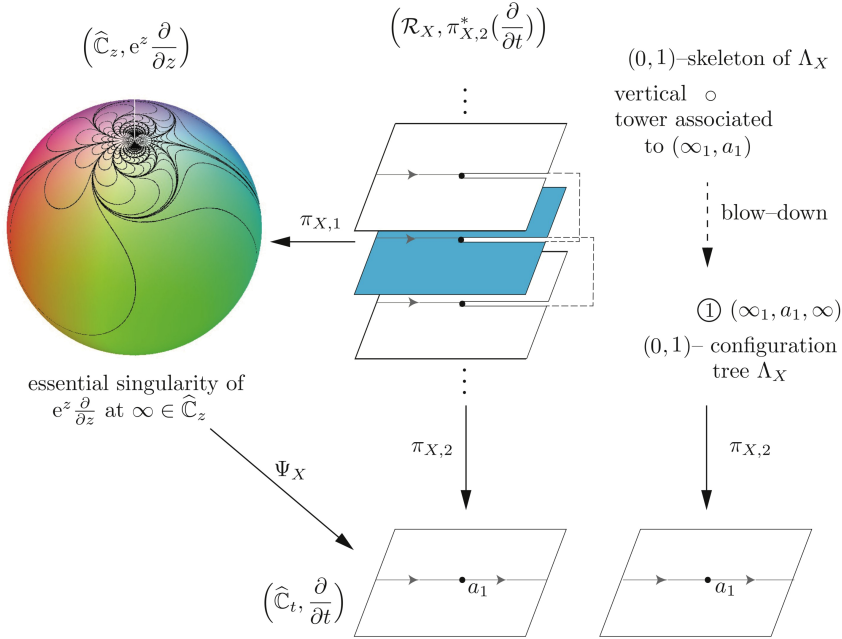


FIGURE 2. Vector field $\lambda^{-1}e^z \frac{\partial}{\partial z}$ with an essential singularity at $\infty \in \widehat{\mathbb{C}}_z$. The surface R_X is a *logarithmic spiral* formed by two semi-infinite helicoids glued together. The soul, Definition 6.2, is shaded blue. See Example 2, and §6.2 for the right drawing.

Example 4. Consider the vector field

$$X(z) = -\frac{e^{z^3}}{3z^2} \frac{\partial}{\partial z}.$$

If $z_0 = 0$ the distinguished parameter is

$$\Psi_X(z) = e^{-z^3} - 1.$$

Thus the pole $p_1 = 0$ has order $-\mu_1 = -2$ and critical value $\tilde{p}_1 = 0$, while the essential singularity at $\infty \in \widehat{\mathbb{C}}_z$ has finite asymptotic value $a_1 = -1$, with multiplicity 3, each corresponding to one of the following exponential tracts

(22)

$$\begin{aligned} A_1 &= \{z \in \mathbb{C} \mid \arg(z) \in [-\pi/6, \pi/6]\}, & A_2 &= \{z \in \mathbb{C} \mid \arg(z) \in [\pi/2, 5\pi/6]\}, \\ A_3 &= \{z \in \mathbb{C} \mid \arg(z) \in [7\pi/6, 3\pi/2]\}. \end{aligned}$$

That is $(\infty_1, -1), (\infty_2, -1), (\infty_3, -1) \in R_X$ are 3 logarithmic branch points corresponding to the above exponential tracts as in Remark 2.

The $(2, 3)$ -configuration tree has three essential vertices, and one pole vertex, which we conveniently renumber as follows

$$\begin{aligned} \textcircled{1} &= (z_1, t_1, \mu_1) = (\infty_1, a_1, \infty), & \textcircled{2} &= (z_2, t_2, \mu_2) = (p_1, \tilde{p}_1, -2), \\ \textcircled{3} &= (z_3, t_3, \mu_3) = (\infty_2, a_1, \infty), & \textcircled{4} &= (z_4, t_4, \mu_4) = (\infty_3, a_1, \infty). \end{aligned}$$

In this way the $(2, 3)$ -configuration tree is

$$(23) \quad \Lambda_X = \left\{ \textcircled{1}, \textcircled{2}, \textcircled{3}, \textcircled{4}; (\Delta_{12}, \lambda_{12}), (\Delta_{23}, \tilde{\lambda}_{23}), (\Delta_{24}, \tilde{\lambda}_{24}) \right\},$$

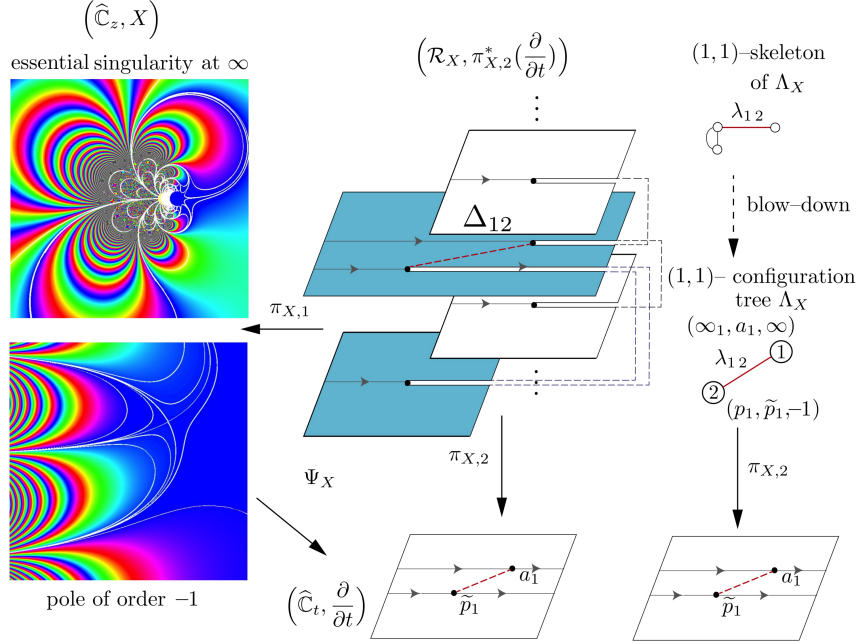


FIGURE 3. Vector field $\frac{e^z}{\lambda(z-p_1)} \frac{\partial}{\partial z}$ with essential singularity at ∞ and simple pole at p_1 . The Riemann surface \mathcal{R}_X consists of two semi-infinite helicoids, and a cyclic helicoid with 2 sheets; the two branch points are the endpoints of the diagonal $\Delta_{12} \subset \mathcal{R}_X$ (coloured red) on the level 0 sheet. The soul, Definition 6.2, is shaded blue. See Example 3, and §6.2 for the right drawing.

with weights given by

$$(24) \quad \begin{aligned} \lambda_{1,2} &= \int_{\infty_1}^{p_1} \omega_X = \tilde{p}_1 - a_1 = 1 \in \mathbb{C}^*, & \tilde{\lambda}_{2,3} &= \int_{p_1}^{\infty_2} \omega_X = -e^{2\pi i} \in \widetilde{\mathbb{C}}^*, \\ \tilde{\lambda}_{2,4} &= \int_{p_1}^{\infty_3} \omega_X = -e^{-2\pi i} \in \widetilde{\mathbb{C}}^*, \end{aligned}$$

the difference in the phases arising from the fact that each exponential tract is on a different sheet on \mathcal{R}_X . See Figure 4 and the left hand side of Figure 6.

Example 5. In a similar vein as the previous example consider the vector field

$$X(z) = \frac{e^{z^3}}{3z^3-1} \frac{\partial}{\partial z},$$

with simple poles at $p_1 = \frac{1}{\sqrt[3]{3}}$, $p_2 = e^{i2\pi/3}p_1$, $p_3 = e^{-i2\pi/3}p_1$, and an essential singularity at $\infty \in \widehat{\mathbb{C}}_z$. Its distinguished parameter is

$$\Psi_X(z) = \int_0^z \omega_X = -ze^{-z^3}.$$

Thus the critical values corresponding to the poles are $\tilde{p}_1 = -\frac{1}{\sqrt[3]{3e}}$, $\tilde{p}_2 = e^{i2\pi/3}\tilde{p}_1$ and $\tilde{p}_3 = e^{-i2\pi/3}\tilde{p}_1$.

The essential singularity at ∞ has $a_1 = 0$ as its finite asymptotic value with multiplicity 3, once again with the same exponential tracts as the previous example, see equation (22), hence $(\infty_1, 0), (\infty_2, 0), (\infty_3, 0) \in \mathcal{R}_X$ are the 3 logarithmic branch points corresponding to the mentioned exponential tracts.

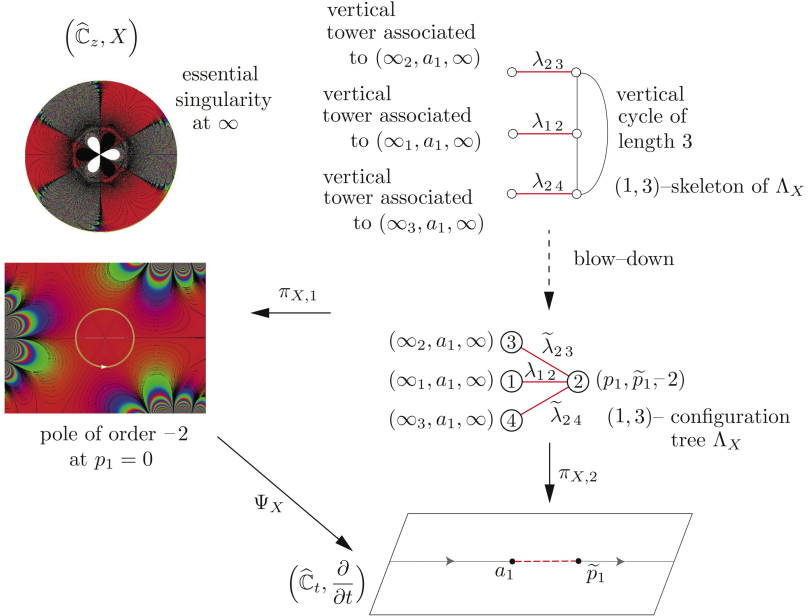


FIGURE 4. Vector field $-\frac{e^{z^3}}{3z^2} \frac{\partial}{\partial z}$ with an essential singularity at ∞ and pole $p_1 = 0$ of order -2 . The projection of the diagonals, Δ_{12} , Δ_{23} and Δ_{24} , onto $\widehat{\mathbb{C}}_t$ is shown in red. The Riemann surface \mathcal{R}_X is not drawn. See Example 4, and §6.2 for the right drawing.

The $(3,3)$ -configuration tree has three essential vertices and three pole vertices, which we renumber conveniently as

$$(25) \quad \begin{aligned} \textcircled{1} &= (z_1, t_1, \mu_1) = (\infty_1, a_1, \infty), & \textcircled{2} &= (z_2, t_2, \mu_2) = (p_1, \tilde{p}_1, -1), \\ \textcircled{3} &= (z_3, t_3, \mu_3) = (p_2, \tilde{p}_2, -1), & \textcircled{4} &= (z_4, t_4, \mu_4) = (p_3, \tilde{p}_3, -1), \\ \textcircled{5} &= (z_5, t_5, \mu_5) = (\infty_2, a_1, \infty), & \textcircled{6} &= (z_6, t_6, \mu_6) = (\infty_3, a_1, \infty). \end{aligned}$$

Thus the $(3,3)$ -configuration tree (see Figure 5) is

$$(26) \quad \Lambda_X = \left\{ \textcircled{1}, \textcircled{2}, \textcircled{3}, \textcircled{4}, \textcircled{5}, \textcircled{6}; \right. \\ \left. (\Delta_{12}, \lambda_{12}), (\Delta_{23}, \lambda_{23}), (\Delta_{24}, \tilde{\lambda}_{24}), (\Delta_{35}, \tilde{\lambda}_{35}), (\Delta_{46}, \tilde{\lambda}_{46}) \right\},$$

with weights given by

$$(27) \quad \begin{aligned} \lambda_{12} &= \int_{\infty_1}^{p_1} \omega_X = \tilde{p}_1 - a_1 = \tilde{p}_1 = -\frac{1}{\sqrt[3]{3e}} \in \mathbb{C}^*, \\ \lambda_{23} &= \int_{p_1}^{p_2} \omega_X = (\tilde{p}_2 - \tilde{p}_1) = \left(\frac{1 - e^{i2\pi/3}}{\sqrt[3]{3e}} \right) \in \mathbb{C}^*, \\ \tilde{\lambda}_{24} &= \int_{p_1}^{p_3} \omega_X = (\tilde{p}_3 - \tilde{p}_1) e^{i2\pi} = \left(\frac{1 - e^{-i2\pi/3}}{\sqrt[3]{3e}} \right) e^{i2\pi} \in \widetilde{\mathbb{C}}, \\ \tilde{\lambda}_{35} &= \int_{p_2}^{\infty_2} \omega_X = (a_1 - \tilde{p}_2) e^{i2\pi} = -\tilde{p}_2 e^{i2\pi} = \left(\frac{e^{i2\pi/3}}{\sqrt[3]{3e}} \right) e^{i2\pi} \in \widetilde{\mathbb{C}}, \\ \tilde{\lambda}_{46} &= \int_{p_3}^{\infty_3} \omega_X = (a_1 - \tilde{p}_3) e^{i2\pi} = -\tilde{p}_3 e^{i2\pi} = \left(\frac{e^{-i2\pi/3}}{\sqrt[3]{3e}} \right) e^{i2\pi} \in \widetilde{\mathbb{C}}. \end{aligned}$$

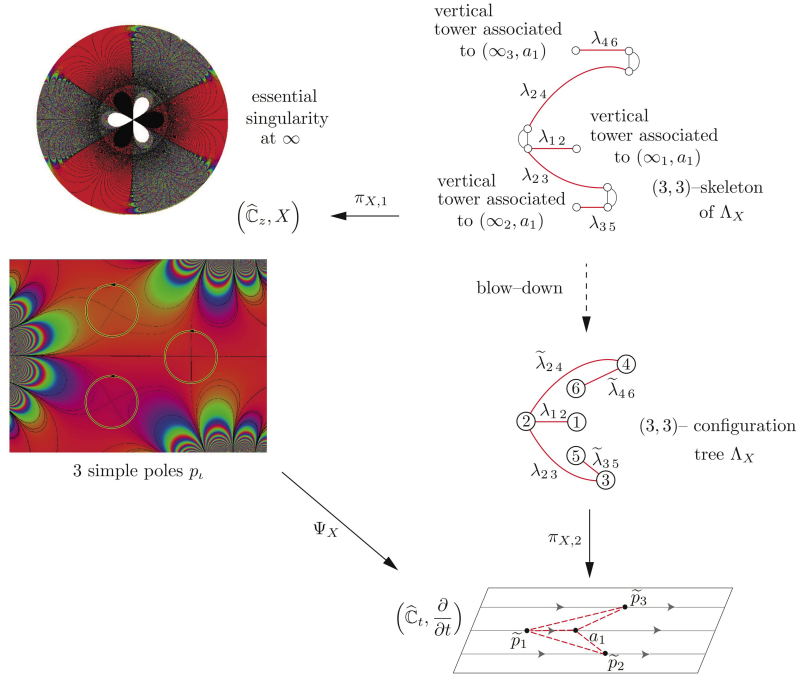


FIGURE 5. Vector field $\frac{e^{z^3}}{3z^3-1} \frac{\partial}{\partial z}$ with an essential singularity at ∞ and 3 simple poles p_i . The projection of the five diagonals onto $\widehat{\mathbb{C}}_t$ are shown in red. The Riemann surface \mathcal{R}_X is not drawn. See Example 5, and §6.2 for the right drawing.

It is instructive to examine in detail how these weights are calculated. The use of Figures 5 and 6 will facilitate the discussion.

For the calculation of the first weight, $\infty_1 \in \overline{\mathbb{C}}_z$ is the starting point for the integration of ω_X , hence $\lambda_{12} = \tilde{p}_1 - a_1 \in \mathbb{C}^*$.

Now consider the calculation of the weight λ_{23} : we seek the value of the integral from p_1 to p_2 , keeping in mind that we have just integrated from ∞_1 to p_1 . The integration path, that goes from ∞_1 through p_1 and then proceeds to p_2 , remains on only two adjacent angular sectors of the pole p_1 (going counterclockwise around the pole p_1 , see Figures 5 and 6 where one can trace the path of integration on the phase plane); which is equivalent to the fact that the image on \mathcal{R}_X of the integration path remains on the same sheet. Hence $\lambda_{23} = \tilde{p}_2 - \tilde{p}_1 \in \mathbb{C}^*$.

Continuing with the weight $\tilde{\lambda}_{24}$, in this case the path of integration, starting from ∞_1 passing through p_1 and ending at p_3 (going counterclockwise around the pole p_1), crosses three adjacent angular sectors of the pole p_1 ; this in turn is equivalent to the fact that the image of the integration path crosses three adjacent half-planes on \mathcal{R}_X , i.e. goes “up” on the ramified surface. Hence $\tilde{\lambda}_{24} = (\tilde{p}_3 - \tilde{p}_1) e^{i2\pi} \notin \mathbb{C}^*$.

For the calculation of $\tilde{\lambda}_{35}$, the integration path must take into account that the previous integration path was coming from p_1 , then the integration continues past p_2 and finally ends at ∞_2 . Since the path crosses three adjacent angular sectors of p_2 then $\tilde{\lambda}_{35} = (a_1 - \tilde{p}_2) e^{i2\pi} \notin \mathbb{C}^*$.

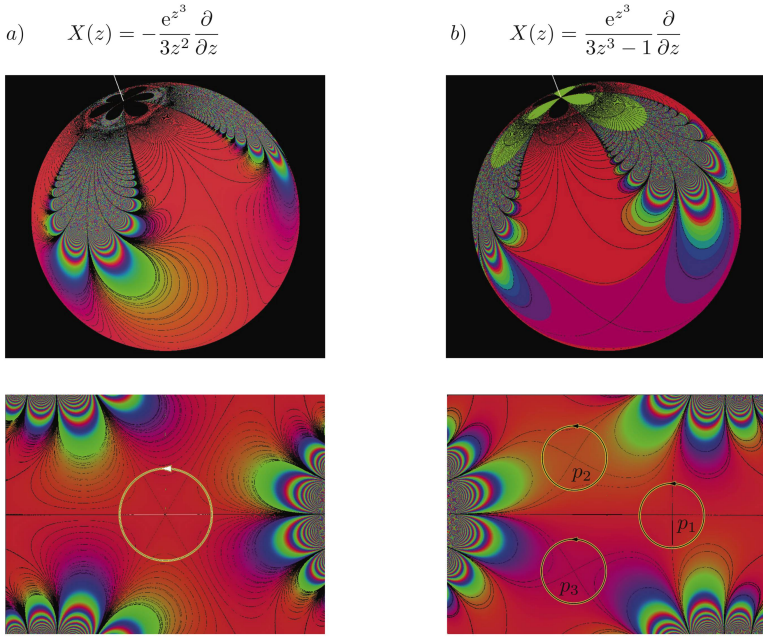


FIGURE 6. Detail of vector fields in Examples 4 and 5. The left hand side shows the vector field $X(z) = -\frac{e^{z^3}}{3z^2} \frac{\partial}{\partial z}$, the right hand side the vector field $X(z) = \frac{e^{z^3}}{3z^3 - 1} \frac{\partial}{\partial z}$. Each angular sector around the poles corresponds to a half plane on \mathcal{R}_X . Note that the dynamics of $\Re(X)$ in a neighbourhood of $\infty \in \widehat{\mathbb{C}}$ are different. The images contain the information needed to construct the corresponding (r, d) -configuration trees, as is explained in the text.

The final calculation, $\tilde{\lambda}_{4,6}$ is the same as the previous one except with p_3 and ∞_3 replacing p_2 and ∞_2 respectively. Thus, once again, $\tilde{\lambda}_{4,6} = (a_1 - \tilde{p}_3) e^{i2\pi} \notin \mathbb{C}^*$.

5.1. Why is classification of $\mathcal{E}(r, d)$ difficult? Let X be in $\mathcal{E}(r, d)$. Recall from section §3, that the graph of Ψ_X is the flat Riemann surface \mathcal{R}_X and in order to specify completely the function Ψ_X , it is necessary to not only specify the finite asymptotic and critical values in \mathbb{C}_t , but also the relative position of the corresponding branch points on \mathcal{R}_X .

Remark 7. In order to get an accurate description, two combinatorial implicit obstacles are the following ones.

D.1 No canonical order can be given to the finite asymptotic and critical values $\{t_a\} \subset \mathbb{C}_t$ of Ψ_X .

D.2 There is no preferred/canonical *horizontal level 0*,

$$\mathbb{C}_{\Delta_{ar}} \setminus \{\text{suitable branch cuts}\} \subset \mathcal{R}_X,$$

that is to be chosen to start the description of \mathcal{R}_X as a combinatorial object.

In particular, note that condition (D.1) will have a repercussion on the enumeration of the vertices in Definition 4.1, while condition (D.2) is associated to the choice of

vertices ① and ③ in the minimality condition of Definition 4.1. Moreover, these difficulties will also arise in the choice of arguments for the diagonals $\tilde{\lambda}_{\alpha\tau} \in \widetilde{\mathbb{C}}^*$, associated to pairs of finite asymptotic or critical values, as will be made explicit in Example 5.

6. PROOF OF MAIN THEOREM: DESCRIPTION OF THE FAMILY $\mathcal{E}(r, d)$ VIA COMBINATORIAL SCHEME

Plan for proof. That $\mathcal{E}(r, d)$ is a complex manifold of dimension $r + d + 1$ is obvious, for a proof in more generality see [2].

For the bijection $\mathcal{E}(r, d) \cong \{[\Lambda_X]\}$: the containment $\mathcal{E}(r, d) \subset \{[\Lambda_X]\}$ is proved in §6.1, and the other containment in §6.2.

The classes of (r, d) -configuration trees will be explained in §6.3.

6.1. From $X \in \mathcal{E}(r, d)$ to an (r, d) -configuration tree Λ_X .

- The trivial case: Ψ_X has exactly one finite asymptotic or critical value:

From Lemma 3.2, only the following two cases are possible,

- 1) $X(z) = \frac{1}{\lambda(z-p)^r} \frac{\partial}{\partial z}$, i.e. $(r, d) = (r, 0)$, or
- 2) $X(z) = \lambda^{-1} e^z \frac{\partial}{\partial z}$, i.e. $(r, d) = (0, 1)$,

where $p \in \mathbb{C}_z$ and $\lambda \neq 0$. Example 2 provides the corresponding Λ_X for (2).

- The non-trivial case: Ψ_X has two or more finite asymptotic or critical values, i.e. $d + n \geq 2$:

Considering the surface \mathcal{R}_X , recall its divisor (17).

1. Vertices of Λ_X .

Let the vertices be the triads obtained from the divisor

$$(28) \quad V = \left\{ (p_\ell, \tilde{p}_\ell, -\mu_\ell) \right\}_{\ell=1}^n \cup \left\{ (\infty_\sigma, a_\sigma, \infty) \right\}_{\sigma=1}^d = \left\{ @ = (z_\alpha, t_\alpha, \mu_\alpha) \right\}_{\alpha=1}^{d+n}$$

There are $d + n$ vertices.

2. Edges of Λ_X . From Definition 3.5, the diagonals, associated to different pairs t_α, t_τ of finite asymptotic or critical values, are *oriented* segments $\Delta_{\alpha\tau} = (z_\alpha, t_\alpha)(z_\tau, t_\tau)$ in \mathcal{R}_X , whose endpoints project down, via $\pi_{X,2}$, to the finite asymptotic or critical values t_α, t_τ . From Lemma 3.6 it follows that there is at least one diagonal associated to each finite asymptotic or critical value. Hence the set of diagonals form the edges of a connected oriented graph.

Note that if a cycle appears on the graph, the branch points corresponding to the vertices in the cycle all lie on the same sheet of \mathcal{R}_X . Such a subgraph will be called a *horizontal subgraph*. Moreover, each horizontal subgraph formed by the set of branch points sharing a same sheet of \mathcal{R}_X , say $\{\ell = (z_\ell, t_\ell, \mu_\ell)\}_{\ell=1}^s$ with $t_1 \geq t_2 \geq \dots \geq t_s$, together with the set of diagonals (edges) forms a complete digraph K_s with $s(s-1)$ oriented edges. However, by eliminating the appropriate edges from K_s we can always obtain an *oriented, traversable, horizontal subtree* such that

$$(29) \quad \begin{aligned} & \text{no branch point } \ell \text{ is in the open horizontal strip} \\ & \pi_{X,2}^{-1}(\{t \in \mathbb{C} \mid \Im(t_j) < \Im(t) < \Im(t_k)\}) \subset \mathcal{R}_X, \\ & \text{defined by any edge } \Delta_{jk}, \text{ in } K_s \text{ whose endpoints} \\ & \text{are not } \ell. \end{aligned}$$

As will become clear (29) will be the *preferred horizontal subtree* condition of Definition 4.1.

On another note, by simple inspection (at least) one of the following cases occur.

$$(30) \quad A) \quad \Delta_{\iota\kappa} = \overline{(p_\iota, \tilde{p}_\iota)(p_\kappa, \tilde{p}_\kappa)}, \quad \pi_{X,2}((p_\iota, \tilde{p}_\iota)) = \tilde{p}_\iota, \quad \pi_{X,2}((p_\kappa, \tilde{p}_\kappa)) = \tilde{p}_\kappa, \\ \text{for some } \iota, \kappa \in \{1, \dots, n\}, \quad \tilde{p}_\iota \neq \tilde{p}_\kappa.$$

$$(31) \quad B) \quad \Delta_{\sigma\iota} = \overline{(\infty_\sigma, a_\sigma)(p_\iota, \tilde{p}_\iota)} \text{ or } \Delta_{\iota\sigma} = \overline{(p_\iota, \tilde{p}_\iota)(\infty_\sigma, a_\sigma)}, \\ \pi_{X,2}((\infty_\sigma, a_\sigma)) = a_\sigma, \quad \pi_{X,2}((p_\iota, \tilde{p}_\iota)) = \tilde{p}_\iota, \\ \text{for some } \sigma \in \{1, \dots, d\}, \iota \in \{1, \dots, n\}, \quad a_\sigma \neq \tilde{p}_\iota.$$

$$(32) \quad C) \quad \Delta_{\sigma\rho} = \overline{(\infty_\sigma, a_\sigma)(\infty_\rho, a_\rho)}, \quad \pi_{X,2}((\infty_\sigma, a_\sigma)) = a_\sigma, \quad \pi_{X,2}((\infty_\rho, a_\rho)) = a_\rho, \\ \text{for some } \sigma, \rho \in \{1, \dots, d\}, \quad a_\sigma \neq a_\rho.$$

We thus obtain a non-weighted, oriented connected traversable tree

$$(33) \quad \left\{ \{\mathfrak{a} = (z_\mathfrak{a}, t_\mathfrak{a}, \mu_\mathfrak{a})\}_{\sigma=1}^{d+n}; \{\Delta_{\alpha\tau}\} \right\}.$$

Without loss of generality, we assume that ① is the starting leaf of the tree.

3. Weights of Λ_X . As an aid, the reader can follow the construction by considering Example 5. [We will include such references inside square brackets.]

For the assignment of weights $\{\tilde{\lambda}_{\alpha\tau}\}$ to the edges $\{\Delta_{\alpha\tau}\}$ we proceed to traverse the tree.

- a) We start to traverse the tree from the starting leaf ①. The edge corresponding to the leaf is $\Delta_{1\mathfrak{z}}$. We define the weight as

$$\tilde{\lambda}_{1\mathfrak{z}} := \lambda_{1\mathfrak{z}} = \overline{(z_1, t_1)(z_\mathfrak{z}, t_\mathfrak{z})} = t_\mathfrak{z} - t_1 \in \mathbb{C}^*.$$

The branch points corresponding to ① and ③ share the same sheet in \mathcal{R}_X . [Referring to Example 5, our first edge is Δ_{12} , and condition (B) is satisfied.]

If we have only two vertices we have completed the construction of Λ_X .

- b) When there are at least 3 vertices, assume we are at the vertex ③, we choose a vertex ④, with $\mathfrak{a} \neq 1, \mathfrak{z}$, such that the edge $\Delta_{\mathfrak{z}\mathfrak{a}}$ exists. The associated weight is defined as in (21) by

$$(34) \quad \tilde{\lambda}_{\mathfrak{z}\mathfrak{a}} = (t_\mathfrak{a} - t_\mathfrak{z}) e^{i2\pi K(\mathfrak{z}, \mathfrak{a})} = |t_\mathfrak{a} - t_\mathfrak{z}| e^{i\arg_0(t_\mathfrak{a} - t_\mathfrak{z}) + i2\pi K(\mathfrak{z}, \mathfrak{a})},$$

where $2\pi K(\mathfrak{z}, \mathfrak{a})$ is the *argument between the sheets*⁵ containing $\Delta_{1\mathfrak{z}}$ and $\Delta_{\mathfrak{z}\mathfrak{a}}$. [Referring to Example 5, the weight $\lambda_{23} \in \mathbb{C}^*$ since on \mathcal{R}_X the diagonals Δ_{12} and Δ_{23} lie on the same sheet; however the weight $\lambda_{24} \in \widetilde{\mathbb{C}^*}$, since on \mathcal{R}_X the diagonals Δ_{12} and Δ_{24} lie on different sheets.]

- c) Continue the assignment of weights as in (b) for all the edges that contain the vertex ③. This exhausts the edges containing the vertex ③.
- d) Continue traversing the tree and assigning the weights as in the previous step until all the vertices are exhausted. [Referring to Example 5, the last edge to be considered is e_{46} with corresponding weight $\tilde{\lambda}_{46} = (a_1 - \tilde{p}_3) e^{i2\pi}$.]

⁵ Geometrically $K(\mathfrak{z}, \mathfrak{a}) \in \mathbb{Z}$ corresponds to the number of sheets in \mathcal{R}_X that separate the diagonals $\Delta_{1\mathfrak{z}}$ and $\Delta_{\mathfrak{z}\mathfrak{a}}$. As is usual language, going around a branch point counterclockwise corresponds to going “upwards” on the ramified surface and hence the number that separates the sheets is positive. Similarly going around the branch point clockwise corresponds to going “downwards”. Furthermore going K times around a finitely ramified branch point of ramification index μ is equivalent to going around it $K \pmod{\mu}$ times.

We have thus constructed an (r, d) -configuration tree

$$(35) \quad \Lambda_X = \left\{ \{\mathfrak{a} = (z_{\mathfrak{a}}, t_{\mathfrak{a}}, \mu_{\mathfrak{a}})\}_{\mathfrak{a}=1}^{d+n}; \{(\Delta_{\mathfrak{a}\mathfrak{r}}, \tilde{\lambda}_{\mathfrak{a}\mathfrak{r}})\} \right\}$$

associated to Ψ_X .

Remark 8. *Non-uniqueness of (r, d) -configuration trees associated to Ψ_X .*

1. There is no canonical way of choosing the non-weighted, oriented connected traversable tree given by (33). This will change the values of $K(\mathfrak{a}, \mathfrak{r})$, and hence of the weights $\tilde{\lambda}_{\mathfrak{a}\mathfrak{r}}$ of the edges of Λ_X .
2. The choice of the weight (in particular the argument) when considering an edge that connects a pole vertex with any other type of vertex is not unique because of the modular arithmetic involved. For instance, if we have an edge $(\Delta_{\mathfrak{t}\mathfrak{r}}, \lambda_{\mathfrak{t}\mathfrak{r}})$ connecting a pole vertex $\mathcal{D} = (p_{\mathfrak{t}}, \tilde{p}_{\mathfrak{t}}, \mu_{\mathfrak{t}})$ to any other vertex \mathcal{C} , then changing $\lambda_{\mathfrak{t}\mathfrak{r}}$ by a factor of $e^{i2\pi(\mu_{\mathfrak{t}}+1)\ell}$ for $\ell \in \mathbb{Z}$, will give rise to a different (r, d) -configuration tree associated to the same Ψ_X .

These issues will be addressed in §6.3.

6.2. From a (r, d) -configuration tree Λ_X to \mathcal{R}_X associated to Ψ_X . In this direction of the proof, we abuse notation by using Λ_X and \mathcal{R}_X instead of Λ and \mathcal{R}_{Λ} .

Let Λ_X be an (r, d) -configuration tree as in (35). The construction will proceed in three steps.

We will first construct the (r, d) -skeleton of Λ_X (a “blow-up” of Λ_X , see Definition 6.1), describing the embedding of Λ_X in $\overline{\mathbb{C}}_z \times \widehat{\mathbb{C}}_t$.

As a second step, from the (r, d) -skeleton of Λ_X we will construct a connected Riemann surface with boundary, the soul of Λ_X (see Definition 6.2).

As the third and final step, we shall glue infinite helicoids on the boundaries of the soul to obtain the simply connected Riemann surface \mathcal{R}_X .

Figure 7 presents a particular example that will help the reader follow the construction.

1. Construction of the (r, d) -skeleton of Λ_X .

The (r, d) -skeleton of Λ_X will contain the same information as Λ_X .

- a) With the disadvantage of being more cumbersome to express.
- b) With the advantage that it will enable us to identify the equivalence classes of Λ_X in §6.3.

First recall that we have two possible types of vertices: essential vertices $\mathcal{O} = (\infty_{\sigma}, a_{\sigma}, \infty)$ and pole vertices $\mathcal{D} = (p_{\mathfrak{t}}, \tilde{p}_{\mathfrak{t}}, -\mu_{\mathfrak{t}})$. Moreover for each weighted edge, $(e_{\mathfrak{a}\mathfrak{r}}, \tilde{\lambda}_{\mathfrak{a}\mathfrak{r}})$, that starts at \mathfrak{a} and ends at \mathfrak{r} , the weight can be expressed as

$$(36) \quad \tilde{\lambda}_{\mathfrak{a}\mathfrak{r}} = \lambda_{\mathfrak{a}\mathfrak{r}} e^{i2\pi K(\mathfrak{a}, \mathfrak{r})}, \quad \lambda_{\mathfrak{a}\mathfrak{r}} \in \mathbb{C}^*, \quad K(\mathfrak{a}, \mathfrak{r}) \in \mathbb{Z}.$$

- I) For each essential vertex $\mathcal{O} = (\infty_{\sigma}, a_{\sigma}, \infty)$, of Λ_X , let

$$K_{\max} = \max_{\mathfrak{r}} \{0, K(\sigma, \mathfrak{r})\} \quad \text{and} \quad K_{\min} = \min_{\mathfrak{r}} \{0, K(\sigma, \mathfrak{r})\},$$

where the maximum and minimum are taken over all the edges that start at \mathcal{O} and end at the respective $\{\mathfrak{r}\}$.

Construct a *vertical tower associated to \mathcal{O}* ; that is an oriented linear graph consisting of exactly $(K_{\max} - K_{\min} + 1)$ copies of the vertex \mathcal{O} joined by $(K_{\max} - K_{\min})$ *vertical edges* (without weights). We shall assign, consecutively, to each vertex of the vertical tower a *level*: an integer starting at $-K_{\min}$ and ending at K_{\max} . Call the increasing direction *up* and the decreasing direction *down*.

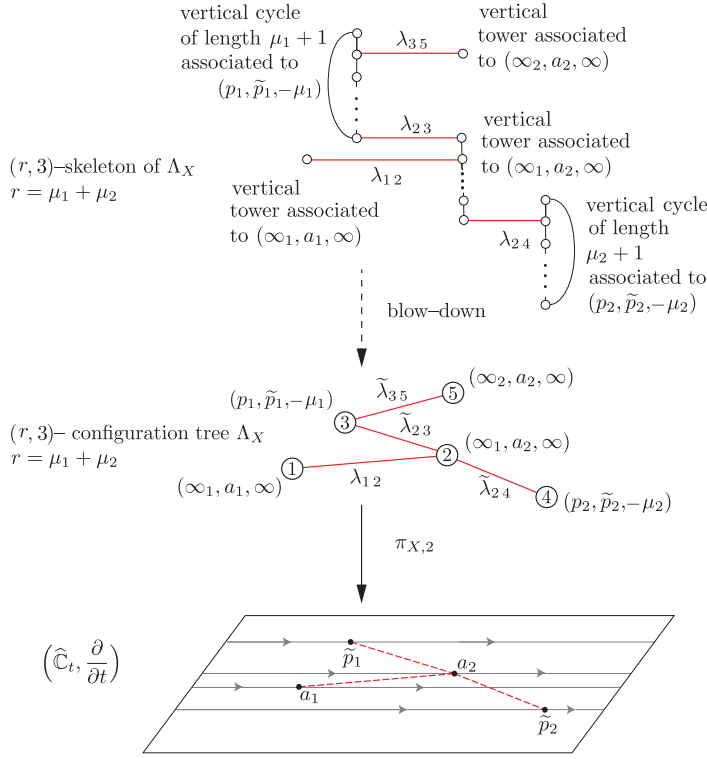


FIGURE 7. $(r, 3)$ -configuration tree Λ_X , $r = \mu_1 + \mu_2$, and its $(3, r)$ -skeleton of Λ_X . To show the possible complexities that arise in the proof of the Main Theorem, we present an example with two poles and 3 finite asymptotic values corresponding to the essential singularity at $\infty \in \widehat{\mathbb{C}}_z$. The vertices are $\textcircled{1} = (\infty_1, a_1, \infty)$, $\textcircled{2} = (\infty_1, a_2, \infty)$, $\textcircled{3} = (p_1, \tilde{p}_1, -\mu_1)$, $\textcircled{4} = (p_2, \tilde{p}_2, -\mu_2)$, $\textcircled{5} = (\infty_2, a_2, \infty)$. The starting vertex is $\textcircled{1}$, with weight $\lambda_{12} = a_2 - a_1 \in \mathbb{C}^*$, while $\tilde{\lambda}_{23}, \tilde{\lambda}_{24}, \tilde{\lambda}_{35} \in \widehat{\mathbb{C}}^*$. The weights $\lambda_{23} = \tilde{p}_1 - a_2$, $\lambda_{24} = \tilde{p}_2 - a_2$, and $\lambda_{35} = a_2 - \tilde{p}_1$ are also elements of \mathbb{C}^* : in the description of the $(3, r)$ -skeleton of Λ_X the information about how many sheets we have gone “up” or “down” the Riemann surface is now included. For instance $\tilde{\lambda}_{23} = e^{i2\pi}\lambda_{23}$ and $\tilde{\lambda}_{35} = e^{i2\pi s}\lambda_{35}$, with $s = -2 \pmod{\mu_1 + 1}$.

The vertical tower will have vertices of valence 1 at the extreme levels $-K_{\min}$ and K_{\max} , otherwise of valence 2. [See vertex $\textcircled{2}$ in Figure 7.]

- II) For each pole vertex $\textcircled{i} = (p_i, \tilde{p}_i, -\mu_i)$, of the original Λ_X , construct a *vertical cycle of length $\mu_i + 1$ associated to \textcircled{i}* ; that is an oriented cyclic graph consisting of exactly $\mu_i + 1$ copies of the vertex \textcircled{i} joined by $\mu_i + 1$ vertical edges (without weights). The vertices on the vertical cycle are also assigned a level: in this case arithmetic modulo $(\mu_i + 1)$ is to be used.

The vertical cycle of length $\mu_i + 1$ will only have vertices of valence 2. Once

again, call one direction of the vertical cycle *up* and the other direction *down*. [See vertex ④ in Figure 7.]

Definition 6.1. The (r, d) -*skeleton* of Λ_X is the oriented graph obtained by:

- a) Replacing each essential and pole vertices with their associated vertical tower or vertical cycle respectively.
- b) The edge, $(e_{\alpha r}, \tilde{\lambda}_{\alpha r}) \in \Lambda_X$, is to end at the level 0 vertex of the vertical tower or vertical cycle associated to ⑩. Furthermore it should start at the level $K(\alpha, r)$ vertex of the vertical tower or vertical cycle associated to ⑨, noting that if ⑨ is a pole vertex, modular arithmetic is to be used.
- c) Finally replace the weights $\tilde{\lambda}_{\alpha r}$ by $\lambda_{\alpha r}$.

Remark 9. The (r, d) -skeleton of Λ_X has the following properties (also see Diagram (37)):

1. The edges of the (r, d) -skeleton of Λ_X are divided in two sets: the vertical edges (alluded to in (I) and (II) above), and

the *horizontal edges* of the form $(e_{\alpha r}, \lambda_{\alpha r})$ with

$$\lambda_{\alpha r} = |t_r - t_\alpha| e^{i \arg_0(t_r - t_\alpha)} \in \mathbb{C}^*,$$

see (21).

2. Consider two horizontal edges $(e_{\beta \alpha}, \lambda_{\beta \alpha})$ and $(e_{\alpha r}, \lambda_{\alpha r})$ in the (r, d) -skeleton of Λ_X that share the vertex ⑨ in the original (r, d) -configuration tree Λ_X . We shall say that:

- The horizontal edge $(e_{\alpha r}, \lambda_{\alpha r})$ is $K(\alpha, r)$ levels *upwards* or *downwards* of the edge $(e_{\beta \alpha}, \lambda_{\beta \alpha})$ in the (r, d) -skeleton of Λ_X depending on whether $K(\alpha, r)$ is positive or negative respectively.
- The edges *share the same horizontal level*, when $K(\alpha, r) = 0$.

Geometrically, $K(\alpha, r)$ can be recognized as

- a) the number of sheets in \mathcal{R}_X separating the diagonals $\Delta_{\beta \alpha}$ and $\Delta_{\alpha r}$ or equivalently
- b) the number of levels in the (r, d) -skeleton of Λ_X separating the edges $(e_{\beta \alpha}, \lambda_{\beta \alpha})$ and $(e_{\alpha r}, \lambda_{\alpha r})$.
3. From the minimality condition the weight $\lambda_{12} \in \mathbb{C}^*$, hence the horizontal subtree containing (e_{12}, λ_{12}) will be called the *horizontal level 0* subtree of the (r, d) -skeleton of Λ_X .
4. By collapsing the vertical edges of the (r, d) -skeleton of Λ_X we (almost) recover the original (r, d) -configuration tree Λ_X . The (r, d) -configuration tree Λ_X is a *blow-down* of the (r, d) -skeleton of Λ_X , see Diagram (37) and Figure 7 for an example.

2. Construction of the *soul* of Λ_X from the (r, d) -skeleton of Λ_X .

It will be convenient to construct an intermediate Riemann surface with boundary, the *soul* of Λ_X (see definition below), before completing the construction of \mathcal{R}_X .

On the (r, d) -skeleton of Λ_X there are two types of vertices; those that do not share horizontal edges and those that share horizontal edges (the vertices that belong to a horizontal subtree).

For simplicity, let us first assume that on any given horizontal subtree the asymptotic and critical values t_r in (28) (associated to these vertices) all lie on different horizontal trajectories of $(\mathbb{C}_t, \frac{\partial}{\partial t})$.

Remark 10. Combinatorial aspects of a sheet arising from the (r, d) -skeleton of Λ_X . We recall Definition 3.3.

Case 1. From a vertex ⑨ with only vertical edges attached to it (there are only two such vertical edges), we obtain a sheet $\mathbb{C}_t \setminus \{L_9\}$ with only one branch cut L_9 .

Note that the two boundaries $[t_a, \infty)_\pm$, of the sheet $\mathbb{C}_t \setminus \{L_a\}$, correspond to the vertical edges.

Case 2. From a horizontal subtree in the (r, d) -skeleton of Λ_X , say with vertices $\{\textcircled{a}_\ell\}$, we obtain a sheet $\mathbb{C}_t \setminus \{L_{a_\ell}\}$. Once again the edges $e_{a_\ell r}$ correspond to the diagonals $\Delta_{a_\ell r} \subset \mathbb{C}_t \setminus \{L_{a_\ell}\}$.

We now start the construction of \mathcal{R}_X from the (r, d) -skeleton of Λ_X .

- a) Replace each vertex⁶ of the (r, d) -skeleton of Λ_X that does not share a horizontal edge with a sheet $\mathbb{C}_t \setminus L_a$.
- b) Given a horizontal subtree with s vertices, say $\{v_\ell\}_{\ell=1}^s$, denote by \textcircled{a}_ℓ the vertex, of the original d -configuration tree, to which the vertex v_ℓ projects down to. Replace the given horizontal subtree with a sheet

$$\mathbb{C}_t \setminus \{L_{a_\ell}\}_{\ell=1}^s,$$

where each L_{a_ℓ} is the horizontal branch cut associated to the vertex \textcircled{a}_ℓ . Since all the values $\{t_{a_\ell}\}$ lie on different horizontal trajectories of $\frac{\partial}{\partial t}$, then none of the horizontal branch cuts L_{a_ℓ} intersect in \mathbb{C}_t .

Continue this replacement process for every horizontal subtree.

Note that we obtain stacked copies of $\mathbb{C}_t \setminus L_a$ and $\mathbb{C}_t \setminus \{L_{a_\ell}\}_{\ell=1}^s$, but they retain their relative position respect to the (r, d) -skeleton of Λ_X , by the fact that we still have not removed the vertical edges of the d -skeleton of Λ_X .

- c) We now replace the vertical towers and vertical cycles in the (r, d) -skeleton of Λ_X with finite helicoids or *cyclic helicoids* respectively (recall Definition 3.4). On each vertical tower or vertical cycle, say the one associated to the vertex \textcircled{a} , glue together the horizontal branch cuts by alternating the boundaries of $\mathbb{C}_t \setminus L_a$, so as to form finite helicoids or cyclic helicoids over the vertex \textcircled{a} , making sure that all the finite helicoids go upwards when turning counter-clockwise around the vertex.

In the case where a vertical tower is involved, the finite helicoid has two boundaries consisting of $[t_a, \infty)_+$ and $[t_a, \infty)_-$; in the case where a vertical cycle is involved we obtain a cyclic helicoid, that is a finite helicoid whose boundaries have been identified/glued.

Definition 6.2. The *soul* of the (r, d) -configuration tree Λ_X is the Riemann surface with boundary described by (a)–(c) above.

Remark 11. The soul is a simply connected Riemann surface that has as boundary d horizontal branch cuts $[a_\sigma, \infty)_- \cup [a_\sigma, \infty)_+$ associated exclusively to the finite asymptotic values $\{a_\sigma\}_{\sigma=1}^d \subset \mathbb{C}_t$.

In particular, for $X(z) = \frac{1}{P(z)} e^{E(z)} \frac{\partial}{\partial z} \in \mathcal{E}(r, d)$ the soul of Λ_X is the Riemann surface \mathcal{R}_{X_0} of $X_0(z) = \frac{1}{P(z)} \frac{\partial}{\partial z} \in \mathcal{E}(r, 0)$ with d branch cuts $\{L_\sigma\}$ at $(\infty_\sigma, a_\sigma)$; here σ enumerates the finite asymptotic values as in (17).

In the particular case when on some horizontal subtree there are at least two asymptotic or critical values $\{t_a\}_{a=1}^{d+n} \subset (\mathbb{C}, \frac{\partial}{\partial t})$ arising from the vertices \textcircled{a} , that lie on the same horizontal trajectory of $\frac{\partial}{\partial t}$. Then by Sard's theorem there is a small enough angle $\theta > 0$ such that the set of values $\{t_a\} \subset (\mathbb{C}, e^{i\theta} \frac{\partial}{\partial t})$ lie on $m + n$ different trajectories of $e^{i\theta} \frac{\partial}{\partial t}$ (in fact any small enough angle $\theta \neq 0$ will suffice).

⁶ Recall that all the vertices of the (r, d) -skeleton of Λ_X are either the original vertices \textcircled{a} of the original (r, d) -configuration tree Λ_X , or copies of them. Thus any vertex in the (r, d) -skeleton of Λ_X projects to a unique vertex on Λ_X .

Proceed with the construction (a)–(e) as above but using $e^{i\theta} L_a$ instead of L_a for the construction. Note that for small enough $\theta > 0$ all the surfaces obtained are homeomorphic. Finally let $\theta \rightarrow 0^+$ and consider the limiting surface.

Example 6. 1) $X \in \mathcal{E}(r, 0)$, so Ψ_X is a polynomial, in which case the soul of Λ_X is \mathcal{R}_X . See Figure 1. The soul is shaded blue in all the figures.

2) $X(z) = e^z \frac{\partial}{\partial z}$, so Ψ_X is an exponential, in which case the soul of Λ_X consists of $\mathbb{C}_t \setminus L_1$, a single sheet with exactly one branch cut. See Figure 2 and figure 11.a in [1].

3) $X(z) = e^{z^2} \frac{\partial}{\partial z}$, so Ψ_X is the error function, in which case the soul of Λ_X consists of $\mathbb{C}_t \setminus (L_1 \cup L_2)$, a single sheet with exactly two branch cuts. See Figure 10 and figure 11.b in [1].

3. Construction of \mathcal{R}_X from the soul of Λ_X . To each of the $2d$ boundaries of the soul of Λ_X , glue a semi-infinite helicoid to obtain a simply connected Riemann surface \mathcal{R}_X . This surface has exactly d logarithmic branch points over d finite asymptotic values and n finitely ramified branch points with ramification indices that add up to $r + n$.

In fact, \mathcal{R}_X is realized via Maskit surgeries with d exp-blocks and r quadratic blocks, hence following M. Taniguchi [23], [24], there exist polynomials $E(z)$ of degree d and $P(z)$ of degree r arising from Λ_X , which characterize the function

$$\Psi_X \in SF_{r,d} = \left\{ \int_{z_0}^z P(\zeta) e^{-E(\zeta)} d\zeta + b \mid P, E \in \mathbb{C}[z], \deg P = r, \deg E = d \right\}.$$

Finally assign to \mathcal{R}_X a flat metric $(\mathcal{R}_X, \pi_{X,2}^*(\frac{\partial}{\partial t}))$ induced by $\pi_{X,2}$. By Proposition 1, our sought after vector field is

$$X(z) = \Psi_X^*(\frac{\partial}{\partial t})(z) = \frac{1}{P(z)} e^{E(z)} \frac{\partial}{\partial z} \in \mathcal{E}(r, d)$$

as required.

Remark 12. An (r, d) -configuration tree has all $K(a, r) \equiv 0$ if and only if on the corresponding Riemann surface \mathcal{R}_X all the diagonals share the same sheet $\mathbb{C}_t \setminus \{L_a\}_{a=1}^{d+n}$.

Remark 13. Note that the (r, d) -configuration tree Λ_X is an abstract graph and, roughly speaking, the (r, d) -skeleton of Λ_X , is a tree “embedded” in \mathcal{R}_X as a subset of $\overline{\mathbb{C}}_z \times \widehat{\mathbb{C}}_t$. It is not a genuine embedding since the branch points of \mathcal{R}_X are replaced by a vertical tower or vertical cycle during the blow-up process of Λ_X (the vertical edges of the (r, d) -skeleton of Λ_X indicate how many sheets separate the diagonals). In this sense, both the (r, d) -configuration tree Λ_X and the (r, d) -skeleton of Λ_X project to a graph $\pi_{X,2}(\Lambda_X) \subset \mathbb{C}_t$. See Figures 1–5 and 7–8, in particular $\pi_{X,2}(\Lambda_X)$ need not be a tree as in Figures 5 and 8. This is represented by the diagram:

$$\begin{array}{ccc}
 \overline{\mathbb{C}}_z \times \widehat{\mathbb{C}}_t & \hookleftarrow & \mathcal{R}_X \text{ “\hookleftarrow” } (r, d)\text{-skeleton of } \Lambda_X \\
 & \updownarrow \text{blow-up} & \updownarrow \text{blow-down} \\
 (37) & & (r, d)\text{-configuration tree } \Lambda_X \\
 & \downarrow \pi_{X,2} & \\
 & & \pi_{X,2}(\Lambda_X) \subset \mathbb{C}_t.
 \end{array}$$

6.3. The equivalence relation on (r, d) -configuration trees.

Definition 6.3. Two (r, d) -configuration trees are equivalent,

$$\Lambda_1 \sim \Lambda_2,$$

if their corresponding (r, d) -skeletons are the same up to:

- 1) Choice of the horizontal level 0 (See §6.1.3.a).
- 2) Relabelling of the vertices (See Remark 8.2).
- 3) Choice of $K(\ell, r)$ on the weight of $\tilde{\lambda}_{\ell r}$ associated to each vertical cycle (occurring when a pole vertex is present). The choice arises because of the modular arithmetic associated to the pole vertex (See Remark 8.3 and Footnote 5).
- 4) Choice of a representative for each horizontal subtree that satisfies the *preferred horizontal subtree* condition of Definition 4.1.

This finishes the proof of the Main Theorem. \square

Following is an examples that illustrate (1), (3) and (4) of the definition.

Example 7. *Choice of horizontal level 0 and of edge to remove when a horizontal cycle occurs.* Let us consider Example 5 once again. Notice that branch points corresponding to the vertices ①, ② and ③ share the same sheet on \mathcal{R}_X , hence the corresponding diagonals form a triangle (a horizontal cycle). Thus there is a choice to be made as to which two diagonals to include in the $(3, 3)$ -configuration tree.

In Example 5, Figure 5, the diagonals chosen are $\overline{(1)(2)}$ and $\overline{(2)(3)}$; if instead we choose $\overline{(1)(2)}$ and $\overline{(3)(1)}$ then we can not start to traverse the tree from vertex ① since ① is not a leaf. This presents us with another choice: to start with vertex ⑤ or vertex ⑥. Choosing to start with vertex ⑤ we obtain the following $(3, 3)$ -configuration tree

$$(38) \quad \Lambda'_X = \left\{ (1, 2, 3, 4, 5, 6; \right. \\ \left. (\Delta_{53}, \lambda_{53}), (\Delta_{31}, \tilde{\lambda}_{31}), (\Delta_{12}, \lambda_{12}), (\Delta_{24}, \tilde{\lambda}_{24}), (\Delta_{46}, \tilde{\lambda}_{46}) \right\},$$

with the parameters given by (27) in Example 5 and

$$\lambda_{31} = \int_{p_2}^{\infty_1} \omega_X = a_1 - \tilde{p}_2 = -\tilde{p}_2 \in \mathbb{C}^*,$$

and $\tilde{\lambda}_{31} = \lambda_{31} e^{i2\pi} \notin \mathbb{C}^*$, since the previous integration path was coming from ∞_2 so the integration path crosses three adjacent angular sectors of p_2 .

Note that since $\lambda_{12} + \lambda_{23} + \lambda_{31} = 0$ then even though the $(3, 3)$ -configuration trees Λ'_X and Λ_X given by (38) and (26), respectively, are not the same, they give rise to the same Riemann surface \mathcal{R}_X . Compare Figures 5 and 8.

7. VIETA'S MAP GENERALIZED TO TRANSCENDENTAL FUNCTIONS

Recall that Vieta's map provides a parametrization of the space of monic polynomials of degree $s \geq 1$ by the roots $\{q_i\}_{i=1}^s$, up to the action of the symmetric group of order s , $S(s)$. Hence by allowing non-monic polynomials $P(z)$ and $E(z)$ in the description of $X \in \mathcal{E}(r, d)$, and recalling the local parameter description of the classes of (r, d) -configuration trees $[\Lambda_X]$, we have.

Proposition 2. $\mathcal{E}(r, d)$ can be parametrized by:

- 1) The $r + d + 2$ coefficients

$$\{(\lambda, b_1, \dots, b_r, c_1, \dots, c_d)\} \subset \mathbb{C}^2 \times \mathbb{C}_{coef}^{r+d}$$

of the polynomials $P(z)$ and $E(z)$.

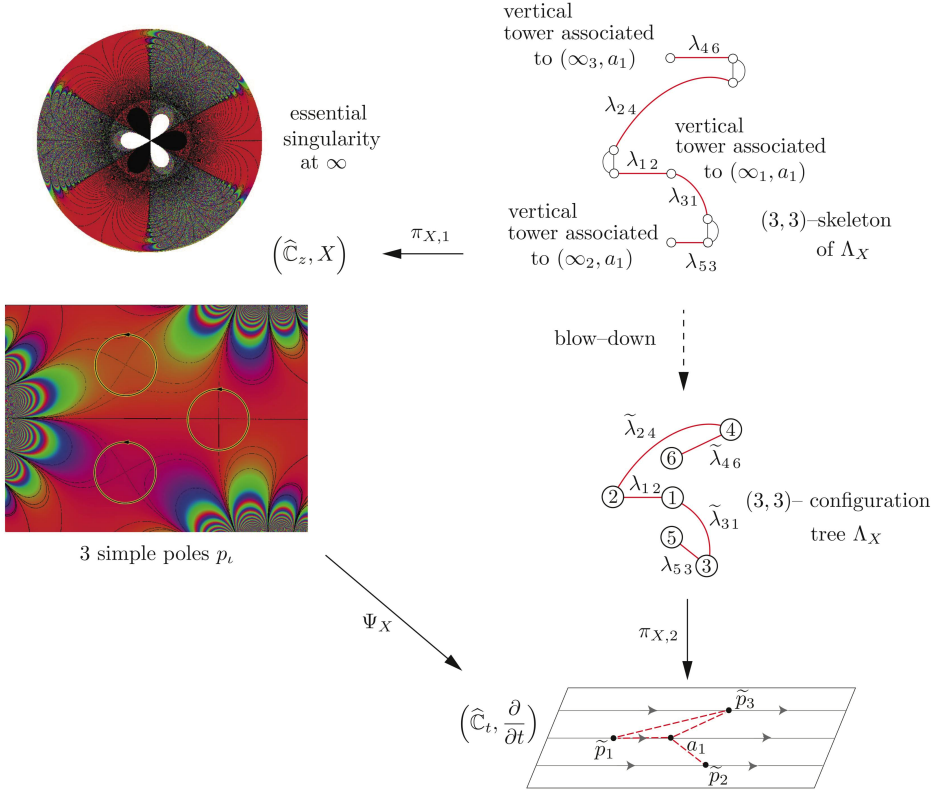


FIGURE 8. **Essential singularity at ∞ (of 1–order 3) and 3 simple poles revisited.** Example 5 revisited. The edge (e_{23}, λ_{23}) was replaced by the edge (e_{31}, λ_{31}) , so as to not produce a cycle $\textcircled{1}\textcircled{2}\textcircled{3}$. Also we now start to traverse the tree from $\textcircled{5}$ since $\textcircled{1}$ is no longer a leaf. The $(3,3)$ –configuration tree is not the same as that of Figure 5. Note that on $(\widehat{\mathbb{C}}_t, \frac{\partial}{\partial t})$ the projection of the diagonal $\Delta_{23} = \overline{\textcircled{2}\textcircled{3}}$ is not present anymore.

- 2) The r roots of $P(z)$, d roots of $E(z)$ and the coefficient λ .
- 3) The $r + d + 1$ local complex parameters $\left\{ z_0, (z_1, t_1, \mu_1), \{\tilde{\lambda}_{\alpha r}\}_1^{r+d-1} \right\}$ defining the classes $[\Lambda_X]$.

Proof. For (1) and (2) see [2].

On the other hand, for (3), note that there are $r + d + 1$ local complex parameters $\left\{ z_0, (z_1, t_1, \mu_1), \{\tilde{\lambda}_{\alpha r}\}_1^{r+d-1} \right\}$ defining the classes $[\Lambda_X]$. All are continuous, and because of the bijection $X \longleftrightarrow [\Lambda_X]$, they form local charts for an atlas of $\mathcal{E}(r, d)$ as a complex manifold of dimension $r + d + 1$. \square

Corollary 1. *There is a complex analytic dependence between*

- 1) the finite critical values and asymptotic values,
- 2) the vertices of Λ_X , and

3) the coefficients of the polynomials $P(z)$ and $E(z)$. □

As an example, in [1], §9.5, the complex analytic dependence for the cases $(r, d) = (0, 1), (0, 2), (0, 3)$ are explicitly computed in terms of the exponential function, the error function and Airy's function respectively.

8. DECOMPOSITION OF THE PHASE PORTRAITS INTO INVARIANT COMPONENTS

Theorem 8.1. *The horizontal strip structure of $X \in \mathcal{E}(r, d)$, into $\Re(X)$ -invariant components, is*

$$(39) \quad (\mathbb{C}_z, X) = \underbrace{\left(\overline{\mathbb{H}}_{\pm}^2, \frac{\partial}{\partial z} \right)}_{4r \geq N_p \geq 2(r+1)} \cup \dots \cup \left(\overline{\mathbb{H}}_{\mp}^2, \frac{\partial}{\partial z} \right) \\ \bigcup_{a_{\sigma}} \left[\left(\left\{ 0 \leq |\Im(z)| \leq 2\pi K_{\sigma} \right\}, e^z \frac{\partial}{\partial z} \right)_{a_{\sigma}} \right. \\ \left. \cup \left(\overline{\mathbb{H}}_{\pm}^2, e^z \frac{\partial}{\partial z} \right)_{a_{\sigma}, up} \cup \left(\overline{\mathbb{H}}_{\pm}^2, e^z \frac{\partial}{\partial z} \right)_{a_{\sigma}, low} \right] \\ \bigcup_{\ell}^{M \leq \infty} \left(\left\{ 0 \leq \Im(z) \leq h_{\ell} \right\}, \frac{\partial}{\partial z} \right),$$

where $\{a_{\sigma}\}$ are the finite asymptotic values of Ψ_X .

Moreover, there are an infinite number of half planes $(\overline{\mathbb{H}}_{\pm}^2, \frac{\partial}{\partial z})$ in the decomposition if and only if $d \geq 1$.

Proof. Decomposition (39) follows by recalling Definition 3.4, the biholomorphism $\pi_{X,1}$ presented in Diagram 3 and the fine structure of the (r, d) -skeleton of Λ_X . It is an accurate description of the phase portrait decomposition of $\Re(X)$:

The first row depicts the, at least $2(r+1)$ and at most $4r$, half planes associated to the r poles.

On the second row are the d finite helicoids arising from the d finite asymptotic values $\{a_{\sigma}\}$, where it is to be noticed that this can be an empty collection.

On the third row are the $2d$ semi-infinite helicoids.

And on the fourth row, the finite height strips associated to the non-horizontal diagonals in \mathcal{R}_X . □

9. ON THE TOPOLOGY OF $\Re(X)$

Consider the group of orientation preserving homeomorphisms

$$Homeo(\mathbb{C})^+ = \{h : \widehat{\mathbb{C}}_z \rightarrow \widehat{\mathbb{C}}_z \mid \text{preserving orientation and fixing } \infty \in \widehat{\mathbb{C}}\}.$$

Definition 9.1. Let $X_1, X_2 \in \mathcal{E}(r, d)$ be two singular analytic vector fields.

They are *topologically equivalent* if there exists $h \in Homeo(\mathbb{C})^+$ which takes the trajectories of $\Re(X_1)$ to trajectories of $\Re(X_2)$, preserving real time orientation, but not necessarily the parametrization.

A *bifurcation* for $\Re(X_1)$ occurs, when the topology of its phase portrait topologically changes under small deformation of X_1 in the family $\mathcal{E}(r, d)$, otherwise X_1 is *structurally stable*, in $\mathcal{E}(r, d)$.

Let $\Lambda_X = \left\{ \{\mathfrak{a} = (z_{\mathfrak{a}}, t_{\mathfrak{a}}, \mu_{\mathfrak{a}})\}_{\sigma=1}^{d+n}; \{(\Delta_{\mathfrak{a}\mathfrak{r}}, \tilde{\lambda}_{\mathfrak{a}\mathfrak{r}})\} \right\}$ be a (r, d) -configuration tree. By simple inspection we have

Theorem 9.2 (Structural stability of $\Re(X)$ for $X \in \mathcal{E}(r, d)$).

The real vector field $\Re(X)$ is structurally stable in $\mathcal{E}(r, d)$ if and only if

- X has only simple poles and

- $\Im(\tilde{\lambda}_{\mathfrak{a}\mathfrak{r}}) \neq 0$ for all weighted edges $\Delta_{\mathfrak{a}\mathfrak{r}}$ of Λ_X . \square

As a direct consequence of the structure of the (r, d) -skeleton of Λ_X we obtain

Theorem 9.3 (Number of topologies of $\Re(X)$ for $X \in \mathcal{E}(r, d)$).

Given a fixed pair (r, d) :

- 1) *The number of topologies of $\Re(X)$ is infinite when*

$$(r, d) \in \{(r \geq 2, 1), (r \geq 1, 2), (r \geq 0, d \geq 3)\}.$$

- 2) *The number of topologies is*

- a) *one when $(r, d) = (0, 1), (1, 0)$;*
- b) *two when $(r, d) = (0, 2), (1, 1)$;*
- c) *bounded above by*

$$3^{(r-1)} \times (r-1) \times r! \times p(r), \quad \text{when } (r, d) = (r \geq 2, 0),$$

where $p(r)$ is the partition function of the integer r .

Let us recall that the phase portrait $\Re(X)$ on \mathbb{C}_z , as in (3) of the theorem, only has a finite number ($\leq r$) of multiple saddle points. These phase portraits were first studied by W. M. Boothby [8], [9], showing that they appear as the real part of certain harmonic functions; in our framework, the imaginary part of $\int \omega_X$.

Proof. The number of topologies can be obtained by looking at the number of possible (r, d) -skeletons of Λ_X associated to the (r, d) -configuration trees.

For each $(r, d) \in \{(r \geq 2, 1), (r \geq 1, 2), (r \geq 0, d \geq 3)\}$ there will be at least one (r, d) -skeleton of Λ_X with at least one vertical tower with two horizontal subgraphs attached to the *same* vertical tower. These horizontal subgraphs are vertically separated from each other by an integer number $K(\sigma, \rho)$, of degree 2 vertices on a vertical tower. Hence there are an infinite number of different ways, described by $\{K(\sigma, \rho) \geq 1\}$, we can attach these two subgraphs to the vertical tower, each of which represents a different configuration in \mathcal{R}_X .

The remaining cases are $(r, d) \in \{(0, 1), (0, 2), (1, 1), (r \geq 1, 0)\}$.

The cases $(0, 1), (1, 0)$ are trivial by Lemma 3.2. For cases $(0, 2)$ and $(1, 1)$: \mathcal{R}_X has two branch points hence they must share the same sheet. Thus each one of these cases have exactly two topologies. Case $(0, 2)$ is illustrated in Figure 10. Case $(r \geq 2, 0)$ corresponds to Ψ_X being a polynomial, hence the number of topologies is finite.

Since poles can have multiplicity, there are $p(r)$ ways of arranging r poles (with multiplicity). Moreover, there are at most $r-1$ diagonals connecting the (at most) r poles. For each diagonal we have at least two and at most three different topologies for $\Re(X)$ (characterized by the diagonal $\Delta_{t\kappa}$: $\Im(t_i) = \Im(t_\kappa)$, $\Im(t_i) < \Im(t_\kappa)$, $\Im(t_i) > \Im(t_\kappa)$). Hence there are at most $3^{(r-1)}(r-1)!$ ways of placing the diagonals on the $(r, 0)$ -configuration tree to obtain a different topology.

Finally we must take into account that each of these diagonals, when viewed on the (r, d) -skeleton of Λ_X , could be at a different level. Let $L(r)$ be the number of ways to place a diagonal on a (r, d) -skeleton of Λ_X . Since there are at most

$r - 1$ diagonals and at most r levels, then a (very rough) upper bound for $L(r)$ is $r(r - 1)$. \square

Table 2 presents a summary of the possible topologies of $\mathfrak{Re}(X)$, for $X \in \mathcal{E}(r, d)$, that arise for different pairs (r, d) .

TABLE 2. Topologies of $\mathfrak{Re}(X)$ for different pairs (r, d) .

r	d	# of topologies of $\mathfrak{Re}(X)$	(r, d) -configuration trees Λ chosen as a representative for the topological class
1	0	1	$\Lambda = \{(p_1, \tilde{p}_1, -1); \emptyset\}$
0	1	1	$\Lambda = \{(\infty_1, a_1, \infty); \emptyset\}$
0	2	2	$\Lambda = \{(\infty_1, a_1, \infty), (\infty_1, a_2, \infty); (e_{12}, \lambda_{12})\}$, with $\lambda_{12} \in \mathbb{C}^*$, two topologies: $\lambda_{12} \in \mathbb{R}, \lambda_{12} \notin \mathbb{R}$
1	1	2	$\Lambda = \{(\infty_1, a_1, \infty), (p_1, \tilde{p}_1, -1); (e_{12}, \lambda_{12})\}$, with $\lambda_{12} \in \mathbb{C}^*$, two topologies: $\lambda_{12} \in \mathbb{R}, \lambda_{12} \notin \mathbb{R}$
2	0	3	$\Lambda = \{(p_1, \tilde{p}_1, -2); \emptyset\}$, gives rise to one topology. $\Lambda = \{(p_1, \tilde{p}_1, -1), (p_2, \tilde{p}_2, -1); (e_{12}, \lambda_{12})\}$, with $\lambda_{12} \in \mathbb{C}^*$, two topologies: $\lambda_{12} \in \mathbb{R}, \lambda_{12} \notin \mathbb{R}$
$r \geq 3$	0	finite see Theorem 9.3 for bound	$\Lambda = \left\{ (p_1, \tilde{p}_1, -\mu_1), \dots, (p_n, \tilde{p}_n, -\mu_n); \right. \\ \left. \{(e_{\iota\kappa}, \lambda_{\iota\kappa}) \mid \iota, \kappa \in \{1, \dots, n-1\}\} \right\},$ $1 \leq n \leq r$ being the number of distinct poles
$r \geq 2$	1	infinite	$\Lambda = \left\{ (\infty_1, a_1, \infty), \right. \\ \left. (p_1, \tilde{p}_1, -\mu_1), \dots, (p_n, \tilde{p}_n, -\mu_n); \right. \\ \left. \{(e_{\mathfrak{a}\mathfrak{r}}, \lambda_{\mathfrak{a}\mathfrak{r}}) \mid \mathfrak{a}, \mathfrak{r} \in \{1, \dots, n+1\}\} \right\},$ $1 \leq n \leq r$ being the number of distinct poles
$r \geq 1$	2	infinite	$\Lambda = \left\{ (\infty_{\alpha_1}, a_1, \infty), (\infty_{\alpha_2}, a_2, \infty), \right. \\ \left. (p_1, \tilde{p}_1, -\mu_1), \dots, (p_n, \tilde{p}_n, -\mu_n); \right. \\ \left. \{(e_{\mathfrak{a}\mathfrak{r}}, \lambda_{\mathfrak{a}\mathfrak{r}}) \mid \mathfrak{a}, \mathfrak{r} \in \{1, \dots, n+2\}\} \right\},$ $1 \leq n \leq r$ being the number of distinct poles
$r \geq 0$	$d \geq 3$	infinite	$\Lambda = \left\{ (\infty_{\alpha_1}, a_1, \infty), (\infty_{\alpha_2}, a_2, \infty), \right. \\ \left. (\infty_{\alpha_3}, a_3, \infty), \dots, (\infty_{\alpha_d}, a_d, \infty), \right. \\ \left. (p_1, \tilde{p}_1, -\mu_1), \dots, (p_n, \tilde{p}_n, -\mu_n); \right. \\ \left. \{(e_{\mathfrak{a}\mathfrak{r}}, \lambda_{\mathfrak{a}\mathfrak{r}}) \mid \mathfrak{a}, \mathfrak{r} \in \{1, \dots, d+n\}\} \right\},$ $0 \leq n \leq r$ being the number of distinct poles

10. EPILOGUE: THE SINGULARITY AT ∞

Our naive question:

how can we describe the singularity of X at $\infty \in \widehat{\mathbb{C}}_z$, for $X \in \mathcal{E}(r, d)$?, is answered in this section.

In [1], §5, germs of singular analytic vector fields X are studied in detail. Starting with a simple closed path γ enclosing⁷ the singularity $z_\vartheta \in \widehat{\mathbb{C}}$, the notion of an admissible cyclic word \mathcal{W}_X in the alphabet $\{H, E, P, \mathcal{E}\}$ is well defined,

$$(40) \quad ((\widehat{\mathbb{C}}, z_\vartheta), X(z)) \longmapsto \mathcal{W}_X.$$

It is to be noted that the affine group $Aut(\mathbb{C})$ is the largest complex automorphism group that acts on $\mathcal{E}(r, d)$,

$\mathcal{A} : Aut(\mathbb{C}) \times \mathcal{E}(r, d) \longrightarrow \mathcal{E}(r, r), \quad (T, X) \longmapsto T^*X,$
see [2]. Hence the germ $((\widehat{\mathbb{C}}, z_\vartheta), X(z))$ is a local analytic invariant.

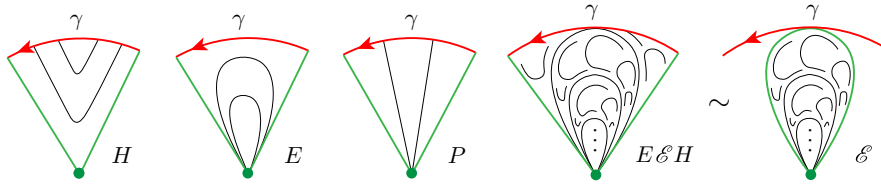


FIGURE 9. Hyperbolic H , elliptic E , parabolic P and entire \mathcal{E} sectors in $\widehat{\mathbb{C}}_z$. The curve γ is shown in red. Note that $E\mathcal{E}H \sim \mathcal{E}$ is illustrated on the right.

The letters in the alphabet are the usual angular sectors for vector fields: hyperbolic H , elliptic E , parabolic P (see [4] p. 304, [5] p. 86) and the new class 1 entire sector \mathcal{E} (see [1] p. 151); see Figure 9.

Specific attributions encoded by the word \mathcal{W}_X in (40) are as follows.

- 1) *Equivalence classes.* The word \mathcal{W}_X is well defined up to the relations
$$E\mathcal{E}H \sim \mathcal{E} \text{ and } H\mathcal{E}E \sim \mathcal{E},$$
 according to [1] pp. 166–167. Under this equivalence the word becomes independent of the choice of the path γ enclosing the singularity.
- 2) *Poincaré–Hopf index.* If the number of letters H , E and \mathcal{E} that appear in a word \mathcal{W}_X at z_ϑ , is denoted by h , e and ε respectively, then the Poincaré–Hopf index formula is

$$PH(X, z_\vartheta) = 1 + \frac{e-h+\varepsilon}{2}.$$

Furthermore, in theorem A p. 130 and §6 of [1], the Poincaré–Hopf index theorem

$$\chi(\widehat{\mathbb{C}}) = \sum PH(X, z_\vartheta)$$

is extended to include germs of singular analytic vector fields X that determine an admissible word.

- 3) *Displacement of parabolic sectors.* As matter of record, each parabolic sector P_ν of \mathcal{W}_X has a displacement number $\nu \in \mathbb{C} \setminus \mathbb{R}$, see [1] pp. 149–150.
- 4) *The residue.* In fact the residue of the word (the vector fields germ) is

$$Res(\mathcal{W}_X) \doteq Res(X, z_\vartheta) = \frac{1}{2\pi i} \int_{\gamma} \omega_X,$$

recall [1] p. 167.

Clearly for $X \in \mathcal{E}(r, d)$ all the residues are zero, since ω_X is holomorphic on \mathbb{C}_z .

⁷ With the usual anticlockwise orientation.

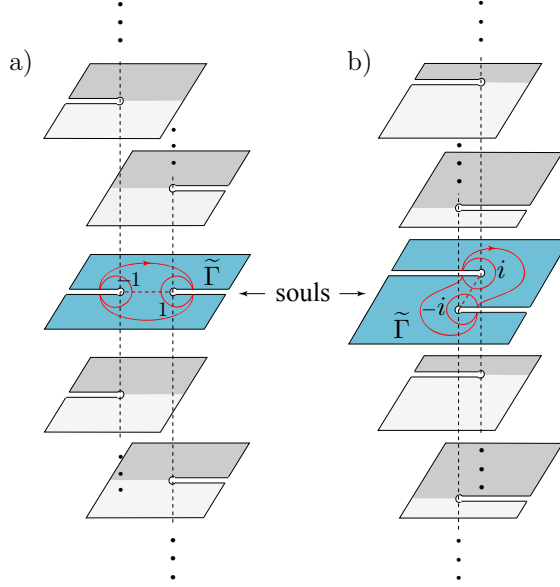


FIGURE 10. Two Riemann surfaces; (a) associated to the error function $\Psi(z) = \frac{2}{\sqrt{\pi}} \int_0^z e^{-\zeta^2} d\zeta$ and (b) to $\Psi(z) = \frac{2i}{\sqrt{\pi}} \int_0^z e^{-\zeta^2} d\zeta$. The red curves represent taut $\tilde{\Gamma}$'s that allow the recognition of the words. The global topologies of the corresponding $\mathfrak{Re}(X)$, $X \in \mathcal{E}(0, 2)$, are described in the third row of Table 2, and the germ of singularities at ∞ in Example 11.

Example 8 (Cyclic words at poles). For a pole $p_\nu \in \mathbb{C}_z$ of order $-\mu_\nu$, the cyclic word \mathcal{W}_X consists of exactly $2(\mu_\nu + 1)$ hyperbolic sectors H :

$$(41) \quad \left((\mathbb{C}_z, p_\nu), X(z) = (z - p_\nu)^{-\mu_\nu} \frac{\partial}{\partial z} \right) \mapsto \mathcal{W}_X = \underbrace{HH \cdots HH}_{2(\mu_\nu + 1)}.$$

The Poincaré–Hopf index of X at p_ν is $-\mu_\nu$.

Example 9 (A cyclic word at ∞). Recall the rational vector field in Example 1, in our language the description of the singularity at infinity is

$$(42) \quad \left((\widehat{\mathbb{C}}_z, \infty), X(z) = \frac{1}{(z - p_1)^{-\mu_1}(z - p_2)^{-\mu_2}} \frac{\partial}{\partial z} \right) \mapsto \mathcal{W}_X = \underbrace{EE \cdots EE}_{\mu_1 + \mu_2 + 2}.$$

The Poincaré–Hopf index of X at ∞ is $\mu_1 + \mu_2 + 2$.

Example 10 (Cyclic words at ∞ having entire sectors). Recall the exponential vector field in Example 2, this basic object produces

$$(43) \quad \left((\widehat{\mathbb{C}}_z, \infty), X(z) = \lambda^{-1} e^z \frac{\partial}{\partial z} \right) \mapsto \mathcal{W}_X = E\mathcal{E}H\mathcal{E} \sim \mathcal{E}\mathcal{E}.$$

The Poincaré–Hopf index of X at ∞ is 2.

Example 11 (The error function). The vector field

$$X(z) = \lambda \frac{\sqrt{\pi}}{4} e^{z^2} \frac{\partial}{\partial z}, \quad \lambda \in \mathbb{C}^*,$$

has associated the error function

$$\Psi(z) = \lambda^{-1} \frac{2}{\sqrt{\pi}} \int_0^z e^{-\zeta^2} d\zeta.$$

Case $\lambda = 1$, the logarithmic branch points are

$$\{(\infty_1, -1), (\infty_2, 1), (\infty_3, \infty), (\infty_4, \infty)\},$$

using the notation in equations (14), and the $\Re(X)$ -invariant decomposition is

$$(\widehat{\mathbb{C}}, X) = \bigcup_{\sigma=1}^{\infty} \left(\overline{\mathbb{H}}_{\sigma}^2, \frac{\partial}{\partial z} \right).$$

The word is

$$\left((\widehat{\mathbb{C}}_z, \infty), X(z) = \frac{\sqrt{\pi}}{4} e^{z^2} \frac{\partial}{\partial z} \right) \mapsto \mathcal{W}_X = E \mathcal{E} H H \mathcal{E} E \mathcal{E} H H \mathcal{E}.$$

See Figure 10.

Case $\lambda = i$, the logarithmic branch points are

$$\{(\infty_1, -i), (\infty_2, i), (\infty_3, \infty), (\infty_4, \infty)\},$$

and the $\Re(X)$ -invariant decomposition is

$$(\widehat{\mathbb{C}}, X) = \left(\bigcup_{\sigma=1}^{\infty} \left(\overline{\mathbb{H}}_{\sigma}^2, \frac{\partial}{\partial z} \right) \right) \cup \left(\{-1 \leq \Im(z) \leq 1\}, \frac{\partial}{\partial z} \right).$$

The word is

$$\left((\widehat{\mathbb{C}}_z, \infty), X(z) = \frac{i\sqrt{\pi}}{4} e^{z^2} \frac{\partial}{\partial z} \right) \mapsto \mathcal{W}_X = E \mathcal{E} H H \mathcal{E} P_{2i} E \mathcal{E} H H \mathcal{E} P_{-2i},$$

note that the appearance of two opposite parabolic sectors having displacements $\pm 2i$ is due the horizontal strip in the decomposition. See Figure 10.

In both cases the Poincaré–Hopf index of X at ∞ is 2.

We now have that for the essential singularity:

Theorem 10.1. 1) Let be $X \in \mathcal{E}(r, d)$, the cyclic word \mathcal{W}_X at ∞ is recognized as

$$(44) \quad ((\widehat{\mathbb{C}}_z, \infty), X) \mapsto \mathcal{W}_X = W_1 W_2 \cdots W_k, \quad W_i \in \{H, E, P, \mathcal{E}\},$$

with exactly $\varepsilon = 2d$ letters $W_i = \mathcal{E}$.

Moreover, $h - e = 2(d - r - 1)$.

2) The word \mathcal{W}_X is a complete topological invariant of a germ $((\widehat{\mathbb{C}}, \infty), X)$.

3) Conversely, a germ of a singular complex analytic vector field $((\mathbb{C}, 0), Y)$ is the restriction of an $X \in \mathcal{E}(r, d)$ at ∞ if and only if the point 0 is an isolated essential singularity of Y and its admissible word \mathcal{W}_Y satisfies that

- i) the residue of the word $\text{Res}(\mathcal{W}_Y) = 0$,
- ii) the Poincaré–Hopf index of the word $PH(Y, 0) = 2 + r$,
- iii) it has exactly $2d$ entire sectors \mathcal{E} .

Proof. The proof of the first statement follows the arguments in §5, §9 and §10 of [1].

Step 1: Take a simple path $\gamma \subset (\widehat{\mathbb{C}}_z, \infty)$ enclosing only ∞ (γ does not enclose any poles of X).

Step 2: Lift γ to Γ in $\mathcal{R}_X \subset \widehat{\mathbb{C}}_z \times \widehat{\mathbb{C}}_t$. Note that Γ lies completely in the soul of \mathcal{R}_X , recall Definition 6.2.

Step 3: The singularity at ∞ of X has a certain self-similarity (as the examples in §5 shown), hence in order to recognize a simple word describing it, a suitable deformation of Γ is required. That is, we deform Γ to a *taut* deformation $\tilde{\Gamma}$ in the soul of \mathcal{R}_X . For examples of a taut deformation $\tilde{\Gamma}$ see Figures 10 and 11. For the appropriate technical definitions and another example see pp. 211–212 of [1], in particular figure 17.

The taut deformation $\tilde{\Gamma}$ recognizes letters W_i at ∞ as follows:

- letters P when $\tilde{\Gamma}$ crosses finite height strip flows,
- letters H when $\tilde{\Gamma}$ makes a half circle around a branch point of \mathcal{R}_X ,
- letters E when $\tilde{\Gamma}$ makes a half circle around (the branch point at) ∞ on a sheet of \mathcal{R}_X ,
- letters \mathcal{E} when $\tilde{\Gamma}$ bounces off the boundaries of the soul of \mathcal{R}_X .

As for the difference $h - e$ between the number of sectors H and E appearing in the cyclic word \mathcal{W}_X at ∞ , we shall use the Poincaré–Hopf index theory extended to these kinds of singularities (theorem A in §6 of [1] with $M = \widehat{\mathbb{C}}_z$).

From the fact that $X \in \mathcal{E}(r, d)$ has exactly r poles (counted with multiplicity) in \mathbb{C}_z and since $PH(X, p_\iota) = -\mu_\iota$ for a pole p_ι of order $-\mu_\iota$, then (6.6) of [1] gives us

$$(45) \quad 2 = \chi(\widehat{\mathbb{C}}) = PH(X, \infty) + \sum_{p_\iota \in \mathcal{P}} PH(X, p_\iota) = PH(X, \infty) - r.$$

On the other hand from (6.5) of [1]

$$PH(X, \infty) = 1 + \frac{e-h+2d}{2},$$

and the result follows.

Assertion (2) follows by simple inspection.

For assertion (3), use a slight modification of corollary 10.1 of [1]. The only change arises from the fact that $X \in \mathcal{E}(r, d)$ has exactly r poles (counted with multiplicity) in \mathbb{C}_z . Once again, by (45) the result follows. \square

Example 12 (Cyclic words at ∞). 1. Recall the vector field in Example 3,

$$(46) \quad \left((\widehat{\mathbb{C}}_z, \infty), X(z) = \frac{e^z}{\lambda(z - p_1)} \frac{\partial}{\partial z} \right) \mapsto \mathcal{W}_X = EP_\nu E\mathcal{E}HH\mathcal{E}P_{-\nu}EE \\ \sim EP_\nu \mathcal{E}H\mathcal{E}P_{-\nu}EE,$$

where $\nu = \tilde{p}_1 - a_1 = -\lambda e^{-p_1}$. Note that if $\nu \in \mathbb{R}$ then $P_{\pm\nu}$ do not appear as letters in \mathcal{W}_X and the word reduces to $\mathcal{W}_X = \mathcal{E}\mathcal{E}EE$.

The Poincaré–Hopf index of X at ∞ is 3.

2. Recall the vector field in Example 4,

$$(47) \quad \left((\widehat{\mathbb{C}}_z, \infty), X(z) = \frac{-e^{z^3}}{3z^2} \frac{\partial}{\partial z} \right) \mapsto \mathcal{W}_X = \mathcal{E}\mathcal{E}\mathcal{E}\mathcal{E}\mathcal{E}\mathcal{E}$$

The Poincaré–Hopf index of X at ∞ is 4.

3. Recall the vector field in Example 5,

$$(48) \quad \left((\widehat{\mathbb{C}}_z, \infty), X(z) = \frac{e^{z^3}}{3z^3 - 1} \frac{\partial}{\partial z} \right) \mapsto \mathcal{W}_X = \mathcal{E}EE\mathcal{E}\mathcal{E}\mathcal{E}\mathcal{E}\mathcal{E}.$$

The Poincaré–Hopf index of X at ∞ is 5.

10.1. The case that all critical and asymptotic values are real. Recall the following result.

Theorem (Eremenko et al., [12], [13]). *If all critical points of a rational function f are real, then f is equivalent to a real rational function.*

This immediately implies that for such a rational function all the critical values are also real.

Motivated by the above, we have.

Corollary 2 (Real critical and asymptotic values).

- 1) If all critical and asymptotic values of Ψ_X for $X \in \mathcal{E}(r, d)$ are in \mathbb{R} , then the following assertions hold.
 - a) \mathcal{R}_X , as in (39), is the union of half planes.
 - b) $\Psi_X : U \subset \widehat{\mathbb{C}} \rightarrow \mathbb{H}^2$ is a Schwartz–Christoffel map, for each half plane U .
 - c) X is unstable in $\mathcal{E}(r, d)$.
- 2) The critical and asymptotic values are in \mathbb{R} if and only if the family of rotated vector fields $\Re(e^{i\theta} X)$ bifurcates at $\theta = n\pi$ for $n \in \mathbb{Z}$.

□

10.2. Relation to Belyi's functions. A rational function is Belyi if it has only three critical values $\{0, 1, \infty\}$, see [6]. We discuss the analogous notion considering asymptotic values.

By Lemma 3.1, we have that for $X \in \mathcal{E}(r, d)$, the distinguished parameter Ψ_X has an even number $2d$ of asymptotic values (counted with multiplicity).

The construction of a $\Psi_X(z)$ having three asymptotic values, say at $\{0, 1, \infty\}$ set theoretically, as in Belyi's theory, is possible for $X \in \mathcal{E}(r, d)$.

Example 13. The vector field $X(z) = \frac{\sqrt{\pi}}{4} e^{z^2} \frac{\partial}{\partial z}$ from Example 11, having associated the error function $\Psi(z) = \frac{2}{\sqrt{\pi}} \int_0^z e^{-\zeta^2} d\zeta$ with logarithmic branch points,
 $\{(\infty_1, -1), (\infty_2, 1), (\infty_3, \infty), (\infty_4, \infty)\}$,

using the notation in Equations (14) and (15). In set theoretically language, its asymptotic values are $\{-1, 1, \infty\}$.

Example 14. A transcendental Belyi function. With the present techniques, we can describe the following example of a vector field arising from a transcendental Belyi function as in [19] p. 292. Let \mathcal{R} be the Riemann surface that consists of half a Riemann sphere (cut along the extended real line $\mathbb{R} \cup \{\infty\} \subset \widehat{\mathbb{C}}$) glued to three semi-infinite towers of copies of $\widehat{\mathbb{C}} \setminus (a, b]$ where $(a, b] \in \{(-\infty, 0], (0, 1], (1, \infty]\}$, as in Figure 11. The general version of the dictionary ([1] Lemma 2.6) shows that a transcendental function $\Upsilon(z) : \mathbb{C}_z \rightarrow \widehat{\mathbb{C}}_t$ and a vector field $X(z) = \frac{1}{\Upsilon'(z)} \frac{\partial}{\partial z}$ are associated to \mathcal{R} .

The (logarithmic) branch points of $\Upsilon(z)$ are

$$\{(\infty_1, 0), (\infty_2, 1), (\infty_3, \infty)\}.$$

Of course there is only one such possible Riemann surface (up to Möbius transformation). Compare also with the line complex description as in p. 292 of [19].

The word is

$$\left((\widehat{\mathbb{C}}_z, \infty), X(z) = \frac{1}{\Upsilon'(z)} \frac{\partial}{\partial z} \right) \longmapsto \mathcal{W}_X = H\mathcal{E}E\mathcal{E}H\mathcal{T},$$

note the appearance of a new word \mathcal{T} that is an angular sector⁸ having an accumulation point of double zeros of X , see Figure 12. The 1-order of X is finite and at least 1.

10.3. Future work.

10.3.1. *Topological classification of $\Re(X)$ for $X \in \mathcal{E}(r, d)$.* As suggested by the results of §9; a careful study of the (r, d) -skeleton of Λ_X allows for a complete topological classification of $\Re(X)$ for $X \in \mathcal{E}(r, d)$, in terms of the placement of the critical and asymptotic values. This will be the subject of future work.

⁸ The phase portrait of $\Re(X)$ is obtained by considering the pullback of $\Re\left(\frac{\partial}{\partial t}\right)$ via Υ .

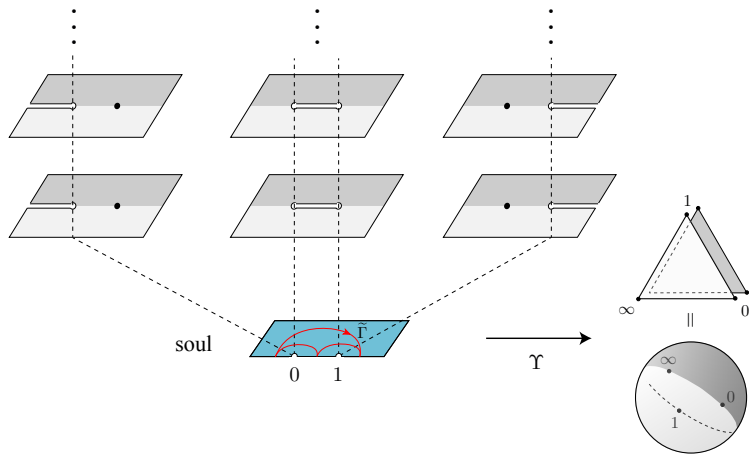


FIGURE 11. Riemann surface corresponding to a transcendental Belyi function Υ . The path $\tilde{\Gamma}$ is the taut deformation of $\Gamma = (\Psi_X \circ \gamma)$ originated by a γ bounding the singularity $((\widehat{\mathbb{C}}, \infty), X_\Upsilon)$. Note that topologically this is the only possible surface with exactly three logarithmic branch points.

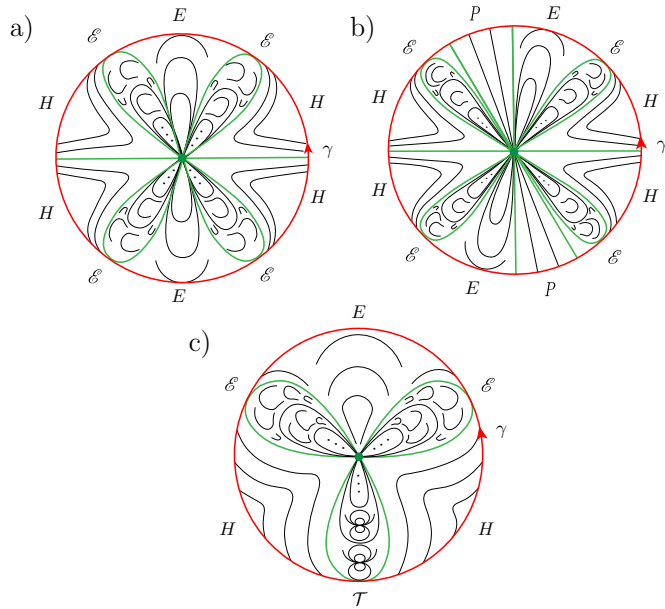


FIGURE 12. The cyclic words (a)–(b) appearing in Examples 11 and (c) in 14. Numerical models for (a)–(b) appeared as figures 15 and 16 in [1].

10.3.2. *Dynamical coordinates for other families of vector fields.* As Example 14 suggests, there are other families of vector fields where the construction of the dynamical coordinates Λ_X is certainly possible.

For instance, when considering the family

$$\mathcal{E}(s, r, d) = \left\{ X(z) = \frac{Q(z)}{P(z)} e^{E(z)} \frac{\partial}{\partial z} \mid Q, P, E \in \mathbb{C}[z], \deg Q = s, \deg P = r, \deg E = d \right\},$$

as in [2], we are presented with two intrinsically different cases:

- 1) If Ψ_X is univalued⁹ then vertices of the form $(q_\ell, \infty, \nu_\ell)$, corresponding to the zeros $Z = \{q_\ell\}_{\ell=1}^s$ of X , need to be added to the description of Λ_X .
- 2) If Ψ_X is multivalued, then extra structure will be required, because of the appearance of logarithmic singularities over those $q_\ell \in \mathbb{C}_z$ where the associated 1-form has non-zero residue.

10.3.3. On cyclic words.

Cyclic words as topological or analytical invariants for germs. The word \mathcal{W}_X (as in Theorem 10.1), is a complete topological invariant of a germ $((\widehat{\mathbb{C}}, \infty), X)$, $X \in \mathcal{E}(r, d)$.

Moreover, the word \mathcal{W}_X in general, is not a global topological invariant of $X \in \mathcal{E}(r, d)$. For example all the vector fields $X \in \mathcal{E}(r, 0)$, $r \geq 3$, with all critical and asymptotic values in \mathbb{R} , have the same word $\mathcal{W}_X = \underbrace{EE \cdots EE}_{2r+2}$ at ∞ .

However, it is possible to modify the definitions of angular sectors P_ν , E and \mathcal{E} so that in fact the corresponding \mathcal{W}_X is a *global analytic invariant* of X modulo $Aut(\mathbb{C})$. This is left for a future project.

Other angular sectors as letters for cyclic words. As shown in Example 14 and in examples 5.9, 5.12 and figures 2, 5 of [1]; there are certainly other possible angular sectors that can be used as letters for cyclic words. In this context and considering the above examples, it is clear that there are an infinite number of topologically different angular sectors (letters) that can appear in a cyclic word associated to an essential singularity for a vector field X .

However, it is not immediately clear *how many topologically different letters there are when we specify the p-order of X* , that is the coarse analytic invariant of functions and vector fields. For instance, by once again considering Example 14, $X(z) = \Upsilon^*(\frac{\partial}{\partial t})(z) = \frac{1}{\Upsilon'(z)} \frac{\partial}{\partial z}$. However we may also consider $Y(z) = \Upsilon^*(\lambda t \frac{\partial}{\partial t})(z) = \lambda \frac{\Upsilon(z)}{\Upsilon'(z)} \frac{\partial}{\partial z}$ which provides a (very) different vector field.

Remark 14. As a side note this shows that the topological classification of functions is coarser the topological classification of phase portraits of vector fields, even for Ψ_X and X in $\mathcal{E}(r, d)$.

REFERENCES

- [1] A. Alvarez-Parrilla, J. Muciño-Raymundo, Dynamics of singular complex analytic vector fields with essential singularities I, *Conform. Geom. Dyn.*, 21 (2017), 126–224. <http://dx.doi.org/10.1090/ecgd/306>
- [2] A. Alvarez-Parrilla, J. Muciño-Raymundo, Symmetries of complex analytic vector fields with an essential singularity on the Riemann sphere, (2019), 25 pages. <http://arxiv.org/abs/1904.11667>

⁹This is equivalent to requiring that the associated 1-form ω_X have all its residues zero.

- [3] A. Alvarez-Parrilla, J. Muciño-Raymundo, S. Solorza and C. Yee-Romero, On the geometry, flows and visualization of singular complex analytic vector fields on Riemann surfaces, To appear in *Workshop in Holomorphic Dynamics*, Inst. de Matemáticas UNAM, 2019 México. <https://arxiv.org/abs/1811.04157>
- [4] A. A. A. Andronov, E. A. Léontovich, I. I. Gordon, A. G. Maier, Qualitative Theory of Second-Order Dynamic Systems, J. Wiley & Sons, New-York, Toronto, 1973.
- [5] V. I. Arnold, Y. Ilyashenko, Ordinary Differential Equations, in Dynamical Systems I, D. V. Anosov, V. I. Arnold Eds., Springer-Verlag, Berlin, 1994.
- [6] G. V. Belyĭ, *On Galois extensions of a maximal cyclotomic field*. Math. USSR Izvestija **193** (1980), no 14, 247–256. <https://doi.org/10.1070/IM1980v014n02ABEH001096>
- [7] W. Bergweiler, A. Eremenko, On the singularities of the inverse to a meromorphic function of finite order, *Revista Matemática Iberoamericana*, Vol 11, No 2, 1995. <http://dx.doi.org/10.4171/RMI/176>
- [8] W. M. Boothby, The topology of regular curve families with multiple saddle points, *Amer. J. Math.*, Vol. 73, No. 2 (Apr., 1951), 405–438. <https://www.jstor.org/stable/2372185>
- [9] W. M. Boothby, The topology of the level curves of harmonic functions with critical points, *Amer. J. Math.*, Vol. 73, No. 3 (Jul., 1951), 512–538. <https://www.jstor.org/stable/2372305>
- [10] R. L. Devaney, *Complex exponential dynamics*, in *Handbook of Dynamical Systems Vol. 3*, B. W. Broer et al. Ed., North-Holland, Amsterdam, 2010, 125–223.
- [11] G. Elfving, Über eine Klasse von Riemannschen Flächen und ihre Uniformisierung, *Acta Soc. Sci. Fennicae*, N.S. 2, Nr. 3 (1934), 1–60.
- [12] A. Eremenko, A. Gabrielov, Rational functions with real critical points and the B. and M. Shapiro conjecture in real enumerative geometry. *Ann. of Math.* (2) 155 (2002), no. 1, 105129. <http://dx.doi.org/10.2307/3062151>
- [13] A. Eremenko, A. Gabrielov, An elementary proof of the B. and M. Shapiro conjecture for rational functions. Notions of positivity and the geometry of polynomials, 167178, Trends Math., Birkhäuser/Springer Basel AG, Basel, 2011. http://dx.doi.org/10.1007/978-3-0348-0142-3_10
- [14] K. Hockett, S. Ramamurti, Dynamics near the essential singularity of a class of entire vector fields, *Transactions of the AMS*, vol. 345, 2 (1994), 693–703. <https://doi.org/10.1090/S0002-9947-1994-1270665-5>
- [15] S. K. Lando, A. K. Zvonkin, *Graphs on Surfaces and Their Applications*, EMS 141, Springer-Verlag (2004). <https://doi.org/10.1007/978-3-540-38361-1>
- [16] H. Masur, S. Tabachnikov, Rational billiards and flat structures, in *Handbook of Dynamical Systems*, Vol. 1A, B. Hasselblatt et al. Ed., North-Holland, Amsterdam, 2002, 1015–1089. [https://doi.org/10.1016/S1874-575X\(02\)80015-7](https://doi.org/10.1016/S1874-575X(02)80015-7)
- [17] J. Muciño-Raymundo, Complex structures adapted to smooth vector fields, *Math. Ann.*, 322, (2002), 229–265. <https://doi.org/10.1007/s002080100206>
- [18] J. Muciño-Raymundo, C. Valero-Valdés, Bifurcations of meromorphic vector fields on the Riemann sphere, *Ergod. Th. & Dynam. Sys.*, 15, (1995), 1211–1222. <https://doi.org/10.1017/S0143385700009883>
- [19] R. Nevanlinna, *Analytic Functions*, Springer-Verlag, (1970).
- [20] R. Nevanlinna, Über Riemannsche Flächen mit endlich vielen Windungspunkten, *Acta Math.*, 58(1), 295–373, (1932). <https://doi.org/10.1007/BF02547780>
- [21] A. Speiser, Über Riemannsche Flächen, *Comment. Math. Helv.*, 2 (1930), 284–293.
- [22] K. Strebel, *Quadratic Differentials*, Springer-Verlag (1984). <https://doi.org/10.1007/978-3-662-02414-0>
- [23] M. Taniguchi, Explicit representations of structurally finite entire functions, *Proc. Japan Acad. Ser. A Math. Sci.*, Vol. 77, (2001), 68–70. <https://projecteuclid.org/euclid.pja/1148393085>
- [24] M. Taniguchi, Synthetic deformation space of an entire function, *Cont. Math.*, Vol. 303, (2002), 107–136. <http://dx.doi.org/10.1090/conm/303/05238>
- [25] W. P. Thurston, *Three-Dimensional Geometry and Topology*. Vol. 1., Princeton University Press, USA (1997).

E-mail address: alvaro.uabc@gmail.com

E-mail address: muciray@matmor.unam.mx